

MODELING CHEMICAL MECHANICAL
PLANARIZATION OF COPPER
WITH AN ATOMIC FORCE MICROSCOPE

THESIS

Presented to the Graduate Council of
Southwest Texas State University
In Partial Fulfillment of
The Requirements

For the Degree
Master of SCIENCE

By

Kelly Fishbeck, B.S.

San Marcos, Texas
August, 2002

ACKNOWLEDGEMENTS

I would like to begin by thanking my family, my mother Mickey and father Robert Fishbeck, and my sister, Casey Leigh. Without their inexhaustible support, both emotionally and financially, I most certainly would not have been able to pursue my studies. Furthermore, I would like express my gratitude to my extended family and friends for their support and patience over the past few years. In particular I would like to acknowledge my closest friends, Jesse Hancock, Connie Hopkins, Houston Ritcheson and Bob Paxton – for helping me keep my focus (and my sanity!) over the past several years. I would also like to express my heartfelt thanks to my wonderful boyfriend, Dereck Todd, for his boundless patience and support during the writing of this thesis.

I would also like to thank all of the faculty members in both the math and physics departments at Southwest Texas. In particular I would like to acknowledge Dr. Terrence McCabe and Dr. Don Hazlewood in the Mathematics Department, Dr. Debbie Koeck in the Chemistry Department, and Dr. James Crawford, Dr. Victor Michalk and Dr. Heather Galloway in the Physics Department. To Dr. Galloway I owe my deepest gratitude, for her patience and belief in me. In addition, I would like to acknowledge all of the students working in Dr. Galloway's laboratory for their help and support, and in particular Kevin Radican for his work on the Magnetron, James McDonald for his work in chemistry and the sample polishing, and Kara Muessig and Mike Arthur for assistance with the AFM. Lastly, I would also like to thank my thesis committee members, Dr. Michalk, Dr. Galloway and Dr. Wilhelmus Geerts for taking the time to help me finish and present my thesis.

August 1, 2002

TABLE OF CONTENTS

ACKNOWLEDGEMENTS.....	iv
LIST OF TABLES.....	vii
LIST OF FIGURES.....	viii

CHAPTER 1 Introduction

1.1	Integrated Circuits and the Semiconductor Industry.....	1
1.2	The Role of Copper in Emerging Technology.....	1
1.3	Related Copper Issues.....	4
1.4	The CMP Process.....	7
1.5	CMP and the Atomic Force Microscope.....	8

CHAPTER 2 The Atomic Force Microscope

2.1	History and Theory.....	11
2.2	Components.....	13
2.3	General Imaging Techniques.....	17
2.4	Forces Involved.....	22
2.5	Modes of Imaging and Related Forces.....	26
	2.5.1 Contact Mode.....	27
	2.5.2 Non-Contact Mode.....	29
	2.5.3 Intermittent Contact.....	31
	2.5.4 Other Methods.....	32
2.6	Calibration.....	34
	2.6.1 X and Y Calibration.....	36
	2.6.2 Z Calibration.....	38
2.7	The Microcell.....	40

CHAPTER 3 Experimental Projects.....42

3.1	Experiment Design.....	42
	3.1.1 Corrosion Inhibitor.....	42
	3.1.2 Corrosive Solutions.....	43
	3.1.3 Abrasive Particles.....	44
	3.1.4 Varying pH.....	45
	3.1.5 <i>Ex Situ</i> vs. <i>In Situ</i>	45
3.2	Ex Situ Studies.....	46
	3.2.1 Procedure.....	46
	3.2.2 Data.....	47
	3.2.3 Discussion.....	54

3.3	In Situ Studies	
3.3.1	Procedure.....	55
3.3.2	Data.....	57
3.3.3	Discussion.....	59
3.4	AFM Tips.....	60
3.4.1	Tip Profiling.....	62
3.4.2	Coated Tips.....	64
CHAPTER 4	Conclusions.....	68
4.1	Comparison of Ex Situ and In Situ Experiments.....	68
4.2	Suggestion for Future Works and Other Projects.....	69
BIBLIOGRAPHY	71
VITA		

LIST OF TABLES

	Page
Table 3.1 This chart displays the RMS roughness, in Angstroms, of 6 copper samples that were polished and then analyzed at sizes of 10, 30 and 80 square microns.....	43
Table 3.2 RMS roughness, in Angstroms, of samples examined ex situ after being polished with solutions buffered to pH 2, pH4, and pH6. Averages are shown in red.....	48
Table 3.3 RMS roughness, in Angstroms, of samples examined ex situ after being polished with solutions buffered to pH 2, pH4, and pH6. Averages are shown in red.....	51
Table 3.4 RMS roughness, in Angstroms, of copper samples studied in situ with the microcell.....	58

LIST OF FIGURES

	Page
Figure 2.1 The Atomic Force Microscope.....	11
Figure 2.2 A magnified view of a typical probe used in the AFM.....	12
Figure 2.3 On the left is a diagram depicting typical dimensions for a cantilever chip, on the right is a magnified view of a tip on one of the triangular protrusions.....	12
Figure 2.4 The white arrow indicates the magnetic disc on which samples are mounted.....	14
Figure 2.5 Diagram of the magnetic sample holder with the piezoelectric tube that is embedded within the scan head.....	15
Figure 2.6 Auxiliary instruments used with the AFM: a) computer with imaging software, b) monitor used to help focus the laser, c) an optical microscope over the AFM head that sends an image to the monitor, d) a floating table, and e) the microscope lid.....	16
Figure 2.7 A red spot on the triangular protrusion to the right indicates that the laser is roughly focused onto the cantilever chip.....	18
Figure 2.8 The imaging software for the AFM, with the two voltmeter windows open. The voltmeter shown at bottom right displays that the A+B signal is about 1.42 Volts, while the voltmeter at the left shows that the A-B signal is about -42 mV.....	19
Figure 2.9 On the left, the laser light bounces off of the back of the cantilever chip and into the photodiode detector. On the right is a diagram of how the motion of the chip is interpreted on the photodiode detector, with the two halves of the detector labeled A and B.....	21
Figure 2.10 On the left, green screen, one of the 256 horizontal line scans is displayed on the x-y plane. On the right, gold screen, a topographical image is being formed, with darker areas indicating lower z-values (crevices) and lighter areas indicating higher z-values (peaks).....	22
Figure 2.11 A meniscus is formed when the thin water layers covering both the tip and sample surface meet.....	24
Figure 2.12 Modes of operation and relative distance to sample.....	27

Figure 2.13 Typical grating used for x and y calibration.....	37
Figure 2.14 AFM image of SrTiO ₃	39
Figure 2.15 On the left is a perspective picture of the microcell attachment for the AFM, on the right is the microcell with the cartridge used to secure it.....	40
Figure 3.1 An example of a copper scan; this particular picture is a 30 micron scan of “as received” copper.....	47
Figure 3.2 Average RMS roughness measured after polishing. Error bars indicate standard deviation. Scan size is one micron square.....	49
Figure 3.3 Average RMS roughness measured after polishing. Error bars indicate standard deviation. Scan size is three microns square.....	49
Figure 3.4 Average RMS roughness measured after polishing. Error bars indicate standard deviation. Scan size is five microns square.....	50
Figure 3.5 Average RMS roughness measured after polishing. Error bars indicate standard deviation. Scan size is ten microns square.....	52
Figure 3.6 Average RMS roughness measured after polishing. Error bars indicate standard deviation. Scan size is thirty microns square.....	52
Figure 3.7 Average RMS roughness measured after polishing. Error bars indicate standard deviation. Scan size is eighty microns square.....	53
Figure 3.8 RMS roughness, in Angstroms, of copper treated in situ.....	58
Figure 3.9 How the tip shape affects the image of the surface.....	61
Figure 3.10 Manufactured surface used for tip profiling.....	62
Figure 3.11 A screen capture image of the tip reconstruction software. Shown clockwise from top left: a top view of the tip profiling surface, a top view of the tip estimation, cross-section of the tip in the x-direction, a 3-D rendering of the tip, and a cross-section of the tip in the y-direction.....	67

CHAPTER ONE

INTRODUCTION

1.1 Integrated Circuits and the Semiconductor Industry

Integrated circuits were developed around 50 years ago, shortly after the invention of the transistor in America in 1947 by John Bardeen, Walter Brittain, and William Shockley¹. Integrated circuits are built on a semiconductor substrate, and are classified by whether they contain either bipolar junction transistors, or metal-oxide-semiconductor (MOS) transistors (some integrated circuits contain both). The number of transistors that are used also classifies integrated circuits, and in the past 15 years, VLSI (very large scale integration) circuits have been developed that contain over 1 million transistors¹. Mainly because of this technology, a very large electronics industry has developed worldwide, with sales of electronic devices reaching hundreds of billions of dollars a year¹.

1.2 The Role of Copper in Emerging Technology

Over the past 30 years, aluminum has traditionally been used to connect the tiny switches in integrated circuits. However, in recent years, new technology is being developed by a number of companies that will likely replace aluminum with copper as the preferred choice for metal interconnects.

One reason that copper is desirable for this purpose is that copper is much less susceptible to electromigration than aluminum. Electromigration is the tendency that metal atoms have to drift when exposed to high current densities¹⁹. Over time, this can create voids and decrease device efficiency. To address this problem, some manufacturers have mixed other metals with the aluminum (including copper)²⁰.

Another important reason for replacing aluminum with copper is that copper is a better conductor of electricity than aluminum, which equates to faster performance and lower required operating power for devices using microprocessors. Copper is a better conductor because, like gold and silver, copper has only one electron in its outer (valence) ring. This means that less energy is required to remove this electron from the copper atom. This “free” electron is now more easily influenced by electrical and magnetic fields, and thus a current flowing through a copper wire (as opposed to aluminum) can travel faster, with less resistance. Since the time delay between interconnects is directly proportional to the product of the resistance of the interconnect material and the capacitance between the interconnects, it follows that switching to a material with less resistance will equate to faster performance speed.

This property makes copper even more important as the current trend in technology requires transistors to become smaller and smaller. The industry ideal has for over a decade strived towards Moore’s Law, which asserts that microprocessor performance should double every 18 months. In recent years this has been achieved in part by shrinking the size of devices, with the feature size of transistors reducing to 0.25 microns, and more recently, 0.18 and even 0.13 microns. As features become closer

together, the capacitance between interconnects increases (capacitance and separation distance are inversely proportional). As has been mentioned, the time delay between interconnects is directly related to capacitance and resistance of the material. Therefore, as the capacitance between materials is increased by bring them closer together, it follows that it is necessary to use a material of lower resistance to lessen the effects that the increased capacitance has on the time delay between interconnects.

The effect of switching to copper technology will ultimately result in producing devices that are smaller, faster, and less expensive. By making the metal interconnects of transistors thinner and shorter, now more than 200 million transistors can be packaged onto a single chip². Because of the increased number of transistors, more data storage space is available for devices. Also because of the superior conductivity of copper, signals traveling through these machines can now move faster with less resistance, improving the overall processing speed. In fact, the speed of some devices has been shown to increase by as much as 40%³. In addition, switching to copper has been estimated to reduce processing costs of some integrated circuits by as much as 30%³. This is due not only to the cost of copper itself, but new ways to process these circuits have been developed commercially that will reduce the production costs even further. The main change in processing involved the fact that copper can not be sputtered onto the wafer surface in the way that aluminum traditionally is. Instead, many manufacturers switched to electroplating the copper, and utilize the “dual damocene” process. This is a process where circuit patterns are dug in trenches onto the wafer, the copper is electroplated onto the surface, and then the etching process removes excess material. It

was found that by switching to this process over traditional methods, the number of steps required for processing could be reduced, and thus reduce processing costs²¹.

Another advantage to using a highly conductive material in integrated circuits is that less power is needed to operate devices that rely on IC technology. Current copper IC's can operate at around 1.8 Volts², making them ideal for battery powered devices such as laptop computers, hand held devices and cell phones. In addition, this lower operating voltage results in microchips that operate at cooler temperatures. Many aluminum-based microchips require that high temperature resistant lead frame alloys be used to create the interface that connects the integrated circuit with other components of the device. By creating a circuit that operates at a lower temperature, new and less expensive alternatives may replace the need for the current lead frame compositions.

1.3 Related Copper Issues

Although the advantages of using copper are numerous, there are also many difficulties that face this new technology. Commercial developments have been made involving new methods of chip manufacture and processing, and investigations have been made concerning new materials for other parts of the chip making process that are complimentary to copper.

One of the first challenges that was faced using copper in integrated circuits is that it is difficult to properly adhere copper to silicon, the most popular substrate used in chip manufacture. In early attempts, the copper had a tendency to diffuse into the silicon, contaminating the device by allowing current to travel in or out of the wrong regions. To confront this problem, several commercial formulas for "diffusion barrier" materials were

developed, and deposited in-between the copper and silicon layer in the transistor³.

Materials used for diffusion barriers include titanium nitride (used by Motorola), tantalum, and tantalum nitride¹⁹.

Another concern with this new technology involves the use of “low-k dielectrics” in conjunction with copper. As integrated circuits get smaller and more compact, not only do feature sizes become smaller, but they are also closer together. As the device shrinks, it has been found that the signal delay at the metal interconnects increases⁴. This is due to the fact that as the metal interconnects are closer to each other, there is more chance of undesirable line to line capacitance. A capacitor is formed when a dielectric material (such as silsequioxane or flourinated silicon oxide⁵) separates two metals (copper interconnects). The amount of charge stored in a capacitor is directly proportional to the dielectric constant (k) of the separating material, and inversely proportional to the separation between metals (line to line distance). The dielectric constant is a property inherent (related to composition) to the material. The choice of a proper dielectric is important, because if the k value of the material is too high, undesirable charge may be stored by these “capacitors”, which in turn limits the operating speed of integrated circuits. This is because the time delay between interconnects is directly related to the capacitance. In fact, these delays have been shown to increase in proportion to the square of the reduction in feature size³. Therefore, as the feature sizes of circuits become smaller, and the features become closer together, the choice of a lower-k dielectric material used to separate metal interconnects in transistors becomes crucial.

One last and very important challenge facing integrating copper into transistors involves a process called Chemical Mechanical Planarization, or CMP. CMP is a process where the metal layers of an integrated circuit are flattened, or planarized, before the next process layer is applied. This is a very important step for several reasons. One is simply that an improperly planarized surface on a lower layer of material will limit the number of additional layers that can be added without distortion. If the surface is rough, and then another layer is deposited, the new layer will model the first and also be uneven. This distortion amplifies with the addition of each new layer, until the exposed surface is too corrugated to build a functional device.

Another reason planarization is important is that in several steps of the transistor manufacture, photolithography is used to mask off different areas of the chip. In this process, a light sensitive chemical (called photoresist) is poured onto the wafer and cured through baking. Then ultraviolet light is projected through a glass mask on which the circuit design is printed. The light passes through the glass except for the areas masked off by chrome plating on the photomask. The photoresist on the wafer is a particular type of material that when exposed to UV light its chemical structure is altered. The exposed areas of photoresist are then processed chemically and removed, leaving the unexposed areas intact to protect parts of the circuit from the next step of processing, which is etching. This step of processing is very important, and with this technique it is possible to build a circuit layer by layer by repeating the process of masking, etching, and deposition. Proper planarization of the wafer is crucial to the photomasking step, because when ultraviolet light is projected through lenses onto the wafer, a rough surface on the wafer can cause focusing problems of the projected image. Areas of the wafer that lie

higher or lower than the intended focal plane of the lenses will be exposed to either less or more light than intended⁶. If this happens, the transistor may not function properly due to materials being deposited, removed, or ionized in the wrong areas. It follows that planarization has become even more important to this step of processing as the feature sizes of these devices decrease.

1.4 The CMP Process

As has been described, Chemical Mechanical Planarization is a crucial procedure in microdevice fabrication. This process is used to remove excess materials deposited on the wafer and also to smooth (or planarize) the surface in preparation for further processing steps. A typical CMP polisher operates by mounting a sample (or wafer) on a rotating head and pressing it against a polishing pad mounted on a platen, which also rotates. During this process, aqueous slurry consisting of corrosive solution and abrasive particles is introduced between the wafer and polishing pad. The solutions and particles used in the slurry vary for different applications, but common solutions used for polishing copper include ammonium hydroxide and nitric acid. Alumina particles are often used for polishing copper, and silica particles are used for polishing many of the low-k dielectrics⁷. These particles are also available in a number of different sizes, and can be used in succession, much like polishing with sandpaper. The surface may be affected by this system in two ways. The mechanical force of the abrasive particles pushing against the surface will either result in the physical removal of metal, or will remove part of a surface film protecting the metal (see corrosion inhibitor, section 3.1.1)⁸. When this film is removed, the metal will then be acted on by the corrosive solution until the protective

film reforms. The speed at which the desired effect is achieved is dependant on a number of variables, including the rotation rate of the wafer and pad, the flow rate of the slurry, the pressure applied between the pad and the wafer, and the pH of the corrosive solution in the slurry⁷.

1.5 CMP and the Atomic Force Microscope

Since planarization is such a necessary step in chip manufacture, finding a way to monitor the effectiveness of this process is important. Often, because there are variations in pressure between the center and outer portions of a wafer, polishing results are not uniform. The layout and varied material composition of wafer layers may also affect the result of the CMP process⁷. Several different methods of study have been used to study the removal rate of material and the remaining feature height of materials at different locations on the wafer.

Two methods that have previously been used to study these types of properties are stylus profilometry and scanning electron microscopy. A stylus profiler works by dragging a stylus probe across a surface and measuring its movement as an indication of surface topography. The disadvantages to this method are that it is limited laterally (cannot profile sub-micron features) and is often damaging to the sample surface⁹. Scanning electron microscopes (SEMs) focus a “probe” of high energy electrons across a surface and relate the intensity of secondary and backscattered electrons to surface composition and topology. The disadvantage to using this method to study wafer properties is that it is often difficult to eliminate the charging of the dielectric materials exposed to electron beam bombardment⁷. In addition, the beam can permanently damage

the material, and it is often necessary to break the wafer to be able to examine feature heights.

Because of these difficulties, the use of the atomic force microscope (AFM) has become more common in studying the effects of CMP. The basic concept of the AFM is somewhat similar to the stylus profilometer, in that a small probe is dragged across the sample surface, and its motion (tracked by a laser) can be interpreted as surface topography. Although the tip used in Atomic Force Microscopy is very sharp, the microscope is capable of scanning at very low forces, thus reducing damaging pressure on the surface. More details concerning the atomic force microscope and the method in which it operates will be discussed in Chapter 2.

Another goal of using atomic force microscopy to study the CMP process is to use the *in situ* (in solution) capabilities of the AFM to simulate the mechanisms of CMP on a microscopic scale. It is hoped that studying the fundamental processes involved in material removal and smoothing will help improve the current CMP techniques. For this simulation, an attachment for the AFM called a microcell (section 2.7) is used to scan a sample surface while exposing it to the corrosive solution used in the polishing slurry. The abrasion of the tip across the sample is comparable to the motion of a single abrasive particle being pushed against a spinning wafer. Similarly to using the large-scale polisher, the effectiveness of this abrasion is dependent on a number of variables, including the size of the particle (AFM tip), exposure time, pressure, and the pH of the corrosive solution. This method has already been used to study the effects of exposing aluminum to chloride solutions, and the tracing of the tip across a small area while in solution resulted in a smooth bottomed trench⁸. Besides the end result, the image

processing capabilities of the AFM software allow a tracking of the process step by step, so that the roughness and grain structure of the metal can be examined mid-process.

Since copper is rapidly replacing aluminum as the material of choice for metal interconnects, it is the goal of this thesis to explore whether the atomic force microscope can be used to study some of the mechanisms of chemical mechanical planarization of copper at the microscopic scale.

CHAPTER TWO

THE ATOMIC FORCE MICROSCOPE

2.1 History and Theory



Figure 2.1 The Atomic Force Microscope.

The Atomic Force Microscope (AFM) is one member of a family of microscopes, collectively referred to as Scanning Probe Microscopes (SPMs). The prototype for the first SPM, called a Scanning Tunneling Microscope (STM), was developed in 1981, by G. Binnig, H. Rohrer, Ch. Gerber, and E. Weibel¹⁰. This microscope was based on the theory of quantum mechanics which predicts that when two electrodes are brought very

close together (on the order of 1 nm), a tunneling current arises that is exponentially dependant on the separation of the electrodes. This type of microscope is useful for obtaining atomic resolution of the electronic structure of surfaces. However it is limited in that the surfaces to be imaged must be composed of a conductive material.

In 1985, G. Binnig, C. F. Quate, and Ch. Gerber designed another type of SPM, called the Atomic Force Microscope, that was capable of lattice and sometimes, atomic resolution for both conductive and insulating materials¹⁰. The AFM maps images by measuring molecular interactive forces between a sample surface and the microscope's atomically sharp probe.



Figure 2.2 A magnified view of a typical probe used in the AFM.

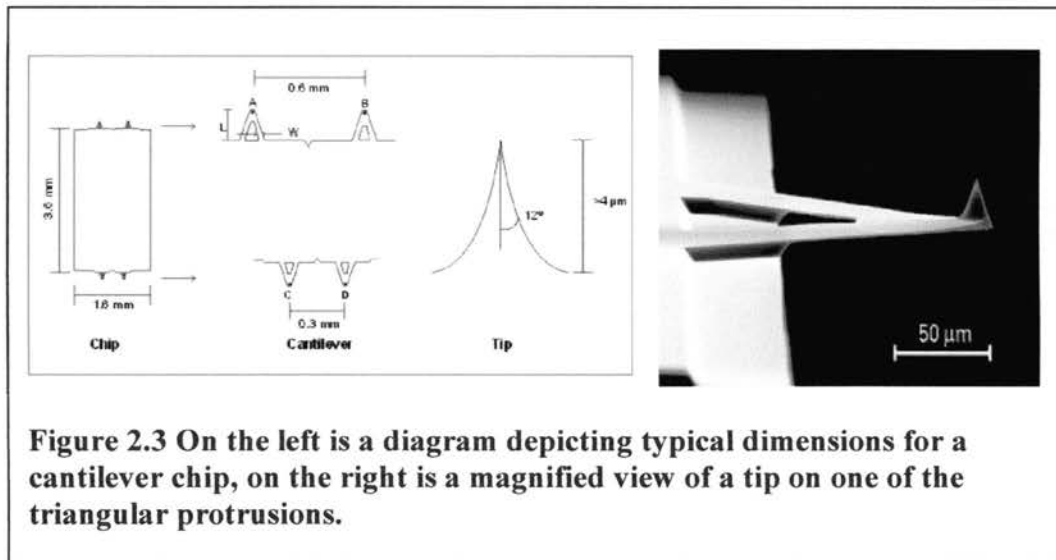
This probe is sharpened to an apex radius of about 10-50 nm, and is mounted onto a soft spring (a “cantilever” with a spring constant ranging from 0.01 to 100 Newtons per meter, depending on the type of imaging that is required). The forces involved in this process will be discussed more in depth on section 2.4. As the sample surface is moved underneath the scanning probe, or tip, a laser is used to record how forces deflect the position of the cantilever. Recording and mapping this interactive force data at regular

intervals can produce a 3-D image of topographic, electronic, and/or magnetic properties of the sample surface.

2.2 Components

An Atomic Force Microscope can be divided into two general sections: the head, which contains the cantilever cartridge, laser and laser detector system; and the body, which contains the sample mount system, and houses the microscope's electronics and input/output interfaces.

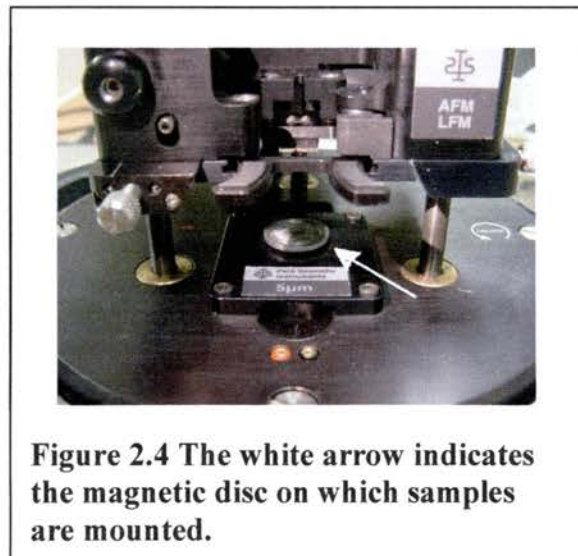
The scanning tips mentioned in the previous section are located at both ends of a tiny manufactured cantilever, at the apexes of small rectangular protrusions.



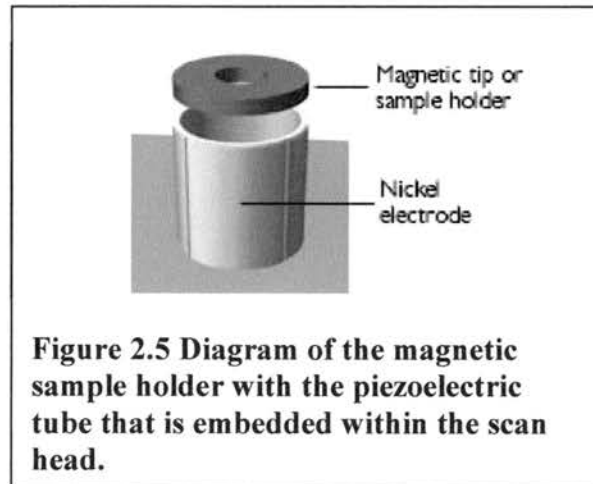
A variety of cantilever choices are available, depending on the mode of operation desired (these modes will be discussed in depth in section 2.5). Cantilever chips can be chosen for their reflectivity, resistivity, spring constants, and tip structure. Typical spring constants are on the order of 0.01 to 100 Newtons per meter. These chips are inserted into

a small rectangular tip holder, which is then secured into a removable cantilever cartridge. Cartridges in the lab are available in two varieties, both for contact and non-contact scanning modes (see section 2.5). Once the cantilever chip is secured, the cartridge is tightened into the head by three screws. Also located within the head are a laser, located to the right of the cartridge, and a photodiode detector, located to the left. This laser is focused onto the back of the cantilever and the photodiode detector is adjusted so that it tracks the motion of the cantilever as it is deflected by properties on the sample surface. On the top left hand side of the head there is an indicator window consisting of four LED indicator lights, which are used to assist the user in laser focusing. A more detailed description of laser focusing and detector adjustment is given in section 2.3.

Below the head, the desired sample is mounted onto the top of a scan head located within the body of the AFM.



There are two types of removable scan heads available in the laboratory, one for large scale (up to 100 micrometers square) scans, and one for small scale (less than 5 micrometers square) scans. At the top of this scan head a small magnetic disk for placing samples is mounted onto a piezoelectric tube. This tube is divided into four quadrants of piezoelectric material.



This material is a polycrystalline ceramic that expands or retracts in the presence of a voltage gradient. An electrode is attached to each quadrant of the tube, as well as one in the interior, which enables the microscope to adjust the tube in the x, y, and z direction. This method of adjustment allows positioning of the sample in relation to the tip with a high level of precision.

There are also a number of auxiliary instruments related with the Atomic Force Microscope in the lab. A computer with imaging software is used to process and display information received from the microscope. The data analysis component of the software allows the user to examine features or properties of images, such as step height, roughness, and grain size and structure. The data presentation component is capable of displaying images in a variety of colors, or in 3-dimensional form from any angle or

scale. Another useful instrument in the laboratory is an optical microscope attached to a video camera that can be moved into position over the microscope head. This signal is displayed by a monitor to the right of the microscope, and is used to assist in fine laser focusing on the back of the cantilever chip. One last and very important component of the microscope setup is the presence of a floating air table on which the microscope is placed. This table is used to help isolate the microscope from physical vibrations in the laboratory. A lid to cover the microscope is also useful in isolating the microscope from periodic vibrations that are produced by other instruments in the lab.

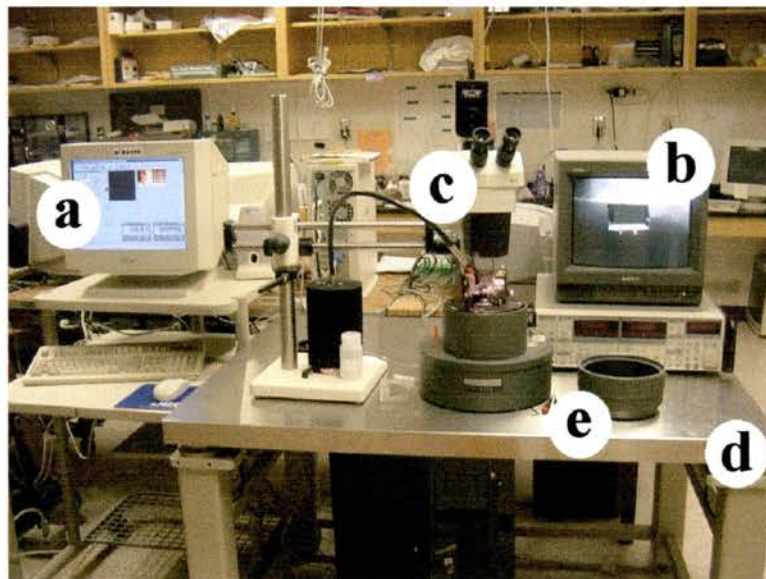


Figure 2.6 Auxiliary instruments used with the AFM: a) computer with imaging software, b) monitor used to help focus the laser, c) an optical microscope over the AFM head that sends an image to the monitor, d) a floating table, and e) the microscope lid.

There are also a number of accessories and tools that are useful to have to work with the samples and various microscope components. Since the samples need to be mounted onto the magnetic sample holder on top of the large piezoelectric tube in the

scan head, small magnetic disks are available on which to adhere the samples. These are available in the lab in two sizes, and samples can be either glued to these or attached using small, double-sided “sticky dots.” The disks are reusable, and can be cleaned with acetone or by rubbing vigorously. A set of plastic tweezers or a small set of pliers can be used to slide the disk onto the magnetic sample holder, and care should be taken when removing or adjusting the sample so that only the disk (and not the magnetic holder on top of the tube) is moved. A small flathead screwdriver is needed to secure or remove the cantilever holder from its mount, and a small allen wrench is needed to adjust the two detector adjustment screws on the front of the machine. Other useful items to have are a small set of tweezers to load the cantilever chips onto the cantilever holder, and a pair of gloves to protect the samples from contamination.

2.3 General Imaging Techniques

After a sample is prepared and mounted on the magnetic sample holder, the first step in obtaining an AFM image is to try to determine what type of imaging technique is best for the experiment. The three most basic modes of imaging are called contact, non-contact and intermittent contact imaging. Each of these methods use different techniques to obtain an image, and a combination of different forces are involved. The applications and methods of each type of imaging are detailed in the sections following this one,

The next step in obtaining an image is to focus the laser on the back of the cantilever and to position the photodiode detector so that it can receive the maximum amount of laser light. To assist in this process, the optical microscope is positioned over the microscope. This microscope can be adjusted in position and magnification, and is

connected to a monitor to provide more convenient viewing. A photograph of the monitor displaying a laser spot focused on a cantilever chip is given below.

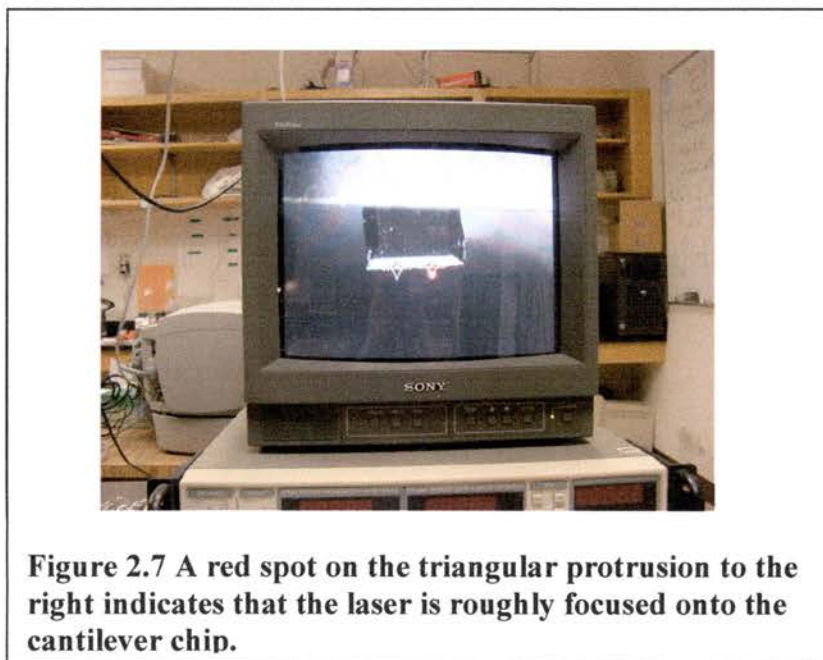
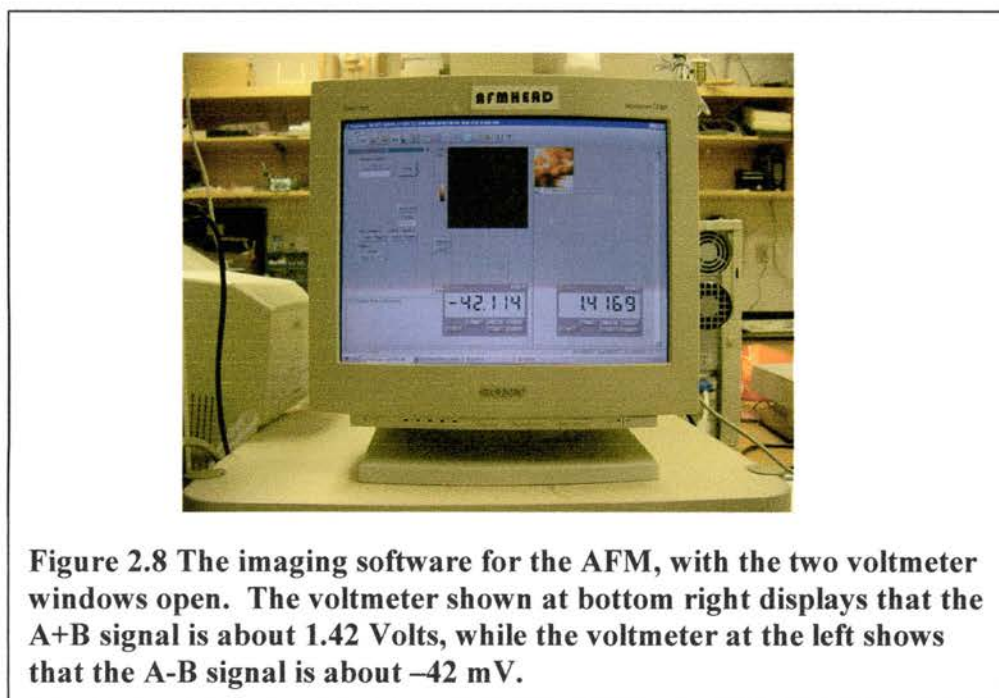


Figure 2.7 A red spot on the triangular protrusion to the right indicates that the laser is roughly focused onto the cantilever chip.

In the Tools menu of the Digital Imaging software, the user should first select to open two small voltmeter screens. One should display the channel “A-B”, and the other “A+B”. The values A and B refer to the two sections of the photodiode detector. The laser position can be adjusted by using the two large screws mounted on top of the microscope head. After the laser is spotted very nearly at the apex of the triangular protrusion of the cantilever chip, the photodiode should be adjusted so that the laser light is fully received by the detector. The detector can be moved up and down by adjusting one of the small hex screws mounted on the front of the machine, and left to right by adjusting the other hex screw. Using a small piece of paper to intercept and view the laser spot shape and size may be useful. After the laser and detector are roughly adjusted, the focus can be finely tuned by observing the A-B and A+B signals on the voltmeter

windows. When the A+B signal is at its maximum (around 1.5-2.0 Volts for general imaging), the laser is sufficiently focused on the back of the cantilever. The A-B signal should be adjusted until it is as close to zero as possible (with a tolerance of about 100 mV). This means that the laser spot is very near the center of the detector.



The laser spot will move during imaging, as the cantilever bends, and the A-B signal will change continuously while imaging. It is important to set it to zero before imaging so that the laser spot will have the full range of motion over the detector while taking an image. To confirm that the proper settings have been achieved, a green light should appear on the position indicator. If any red lights appear, the laser and detector should be adjusted.

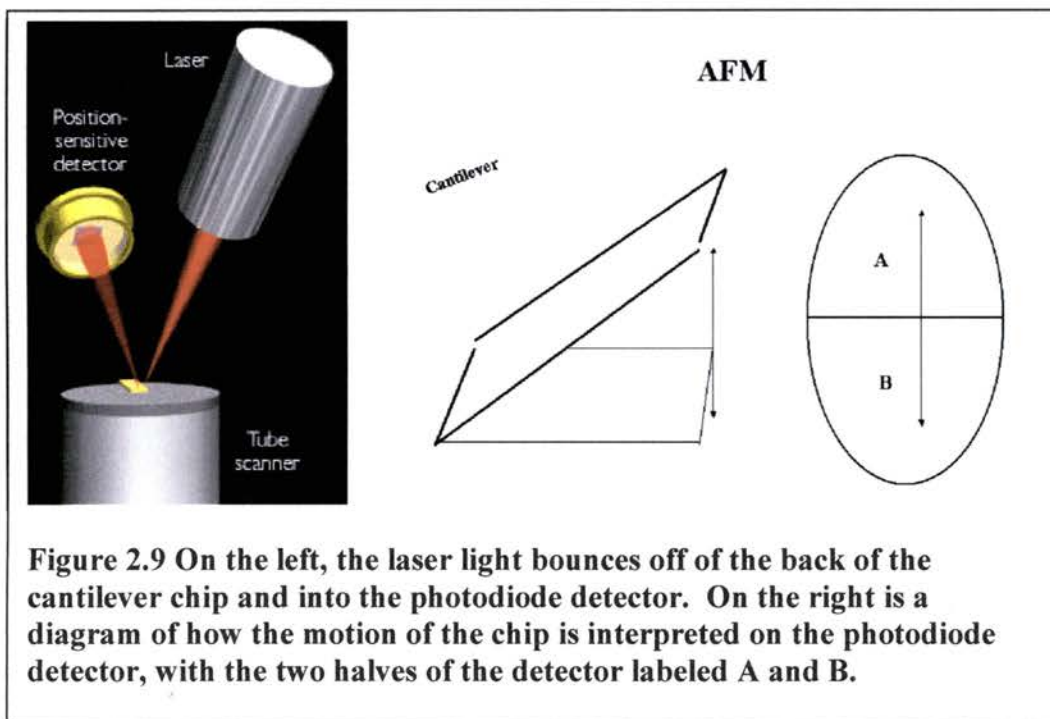
After the tip is in range of the sample, the imaging software then allows the user to enter the specifics of the desired scan, including scan size, scan rate, and setpoint

force. On the left side of the computer screen, a line scan reflecting a single line of data is shown. At this time the software allows adjustment of the slope of this line in both the x and y directions. This is an important step in obtaining a clear AFM image, to ensure that the vertical range of the scan does not exceed the machine capabilities. As the slope value is adjusted, the software applies voltages to different quadrants of the piezoelectric tube on which the sample is mounted. Thus it is possible to adjust the scan direction to match the plane of the sample so that it is as perpendicular to the tip as possible.

It is also useful at this time to adjust the “gain” of the electronic feedback loop that keep the tip and sample at the proper distance needed to maintain the setpoint force between them. If the gain is set too high, a distinct oscillation can be seen on the line image. The gain is related to the speed at which the tip reacts to features on the sample surface. If the tip moves too quickly, the tip may respond too strongly and overcompensate, causing the cantilever to vibrate strongly. This phenomenon is viewed on the line scan as sharp oscillations that do not model the surface structure. Setting the gain too low results in a “smoothing” of the image, as the tip reacts too slowly to surface features. Since the gain governs how quickly the tip reacts to features, and the setpoint force ultimately governs the distance between the tip and sample, it should be noted that it is sometimes useful to lower the setpoint force as the gain is increased (and visa versa).

After the proper scan parameters are obtained, an image can be obtained by pressing the “IMAGE” button on the AFM software. The AFM moves the sample horizontally underneath the tip, over an area designated by the selected scan size. As the sample moves underneath the tip, the tip cantilever bends in response to the surface

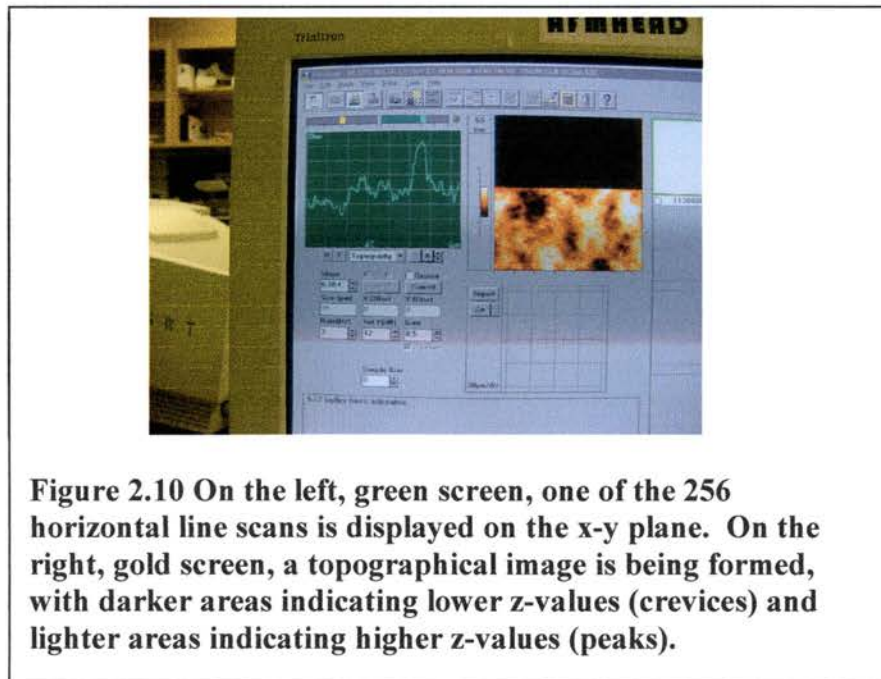
topography. The laser light bouncing off of the back of the cantilever is deflected and thus the laser spot shifts on the photodiode detector.



The amount that the laser light is deflected is measured by the difference in intensity of light on the two sectors of the detector (denoted A and B). This is interpreted by the software as a voltage difference (A-B signal), and a voltage to distance ratio is applied (to be discussed in the Calibration Section 2.6). This distance measurement in turn is used to determine voltages to apply to different sectors of the piezoelectric tube so that the sample can once again be extended or retracted to settle at the proper distance to maintain the setpoint force. Thus the scanner's z-motion is used to map the topography.

The entire process is very quick, and is repeated for a total of 256 times for each line. A total of 256 lines with 256 data points each are taken over the area, for a total of 2^{16} data points. The computer software then arranges the data points on the image screen

by assigning a color to each “height” on the surface. In this way a 2-D image is formed that maps the surface topography.



2.4 Forces Involved

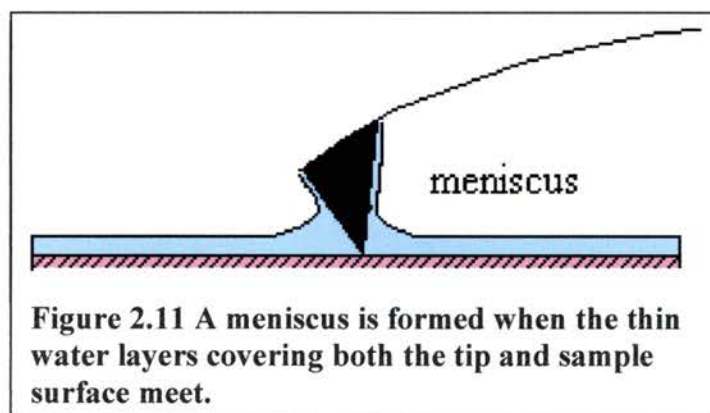
The fundamental principle that enables Atomic Force Microscopy to work is that when a sharp tip mounted on a weak spring is brought very close to a surface, atoms at the edge of the tip experience forces due to both the scan environment and the surface topography. It should also be noted that similarly, the surface experiences forces due to the proximity of the tip. It is possible to monitor these forces, using the laser and detector system to track the motion of the spring. This data, in turn, can be used to infer surface properties of the sample, such as topography, composition, or the location of magnetic or electrically charged regions. As the tip approaches the sample, these forces vary at different distance intervals, in both strength and the number of forces involved. Some of these forces arise from conditions in the environment in which the tip-sample system is

immersed. Such environments include using the equipment in air, in liquid, or in vacuum. Other forces are due to the proximity of the atoms on the surface of both the tip and the sample. These forces can be either repulsive or attractive, and are of both electrical and magnetic origin. The three primary forces involved when the tip-sample system is used in air are the van der Waal's force, the meniscus force, and electron interaction forces.

A group of forces called the van der Waal's forces is one of the forces affecting the system, and contributes to the deflection of the tip-spring when the separation of tip and sample is between one to several tens of nanometers¹¹. These forces arise from interactions between molecules on the sample surface and the tip, and arise for a variety of reasons. The tip and sample molecules may be permanently polarized, or a polarized molecule may induce a dipole moment in a previously neutral molecule. Also, neutral molecules have fluctuating multipole moments at very short time intervals¹¹. All of these forces result in an attractive force being created between the tip and the sample. This attractive force is distance dependent, and the relationship is best described by examining the forces due to fluctuating dipole moments. These forces are the most dominant of the three van der Waal's forces in most cases, and are called dispersion forces. This fluctuating orientation of charge creates an electric field around the dipole moment that is distance dependent, and inversely proportional to the cube of the distance from the dipole¹². A second molecule polarized by this field has an induced dipole moment also inversely proportional to the cube of the distance from the first molecule. Taking into account both dipoles and their orientation, it follows that the attractive force between the two molecules is inversely proportional to the sixth power of the distance between them.

The attractive van der Waal's forces are the main forces affecting the tip-sample system until separation nears a few Angstroms.

Another attractive force present when the system is used in air is called the meniscus force. When the tip and sample are exposed to the air, a thin layer of water condenses on the surface. The thickness of this layer is dependent on the temperature, humidity and sample material. When the tip is very near the sample, the two water layers meet and a meniscus is formed.



The high surface tension of water pulls the tip and sample together, and when the two layers first meet this is often characterized by the tip quickly “snapping” into range. This force is usually in the range of ten to hundreds of nanoNewtons, and is significant at separation distances of one to around twenty nanometers. Since this effect is nearly impossible to eliminate in air, it should be noted that the meniscus force can often be limiting in AFM. In many cases it is desirable to image at very low forces, to minimize damage to the sample material. The meniscus force then serves to limit the lowest value at which scanning can be achieved. Since this is an environmental limitation, many

experiments have been successful at eliminating this concern by imaging either in vacuum or in liquid.

As the tip and sample get extremely close (within a few Angstroms), the attractive van der Waal's and meniscus forces are overpowered by a repulsive force due to the electron cloud interactions of the two surfaces. These forces can be interpreted both macroscopically and in quantum mechanical terms. In classical terms, the two clouds of electrons approaching each other can be modeled as being two distinct bodies, each with net negative charge. These two negative distributions repel each other, with a force that is distance dependant. Another way to model this effect is to use the Pauli Exclusion Principle. This principle states that for fermions (electrons), "no two fermions in an atom can have the same quantum number"¹³. What this physically translates to is that no two electrons can occupy the same state at the same time. This results in a repulsive force due to the electron cloud overlap of molecules separated by less than a bond length (less than 2-3 Angstroms). At this range, this force is strong enough to dominate over other attractive forces felt by the system.

It should be noted that if the sample exhibits other types of magnetic or electric properties, the tip may experience some force due to these fields as well. This process can be enhanced by either coating the tip with a magnetic material or electrically charging the tip. Besides vertical forces, if the tip is used in contact mode (within a few Angstroms of the surface, or touching the surface), the tip will also experience lateral (frictional) forces due to both the topography and composition of the surface. All of these forces combine to cause the tip to move up and down and twist as the scanner traces

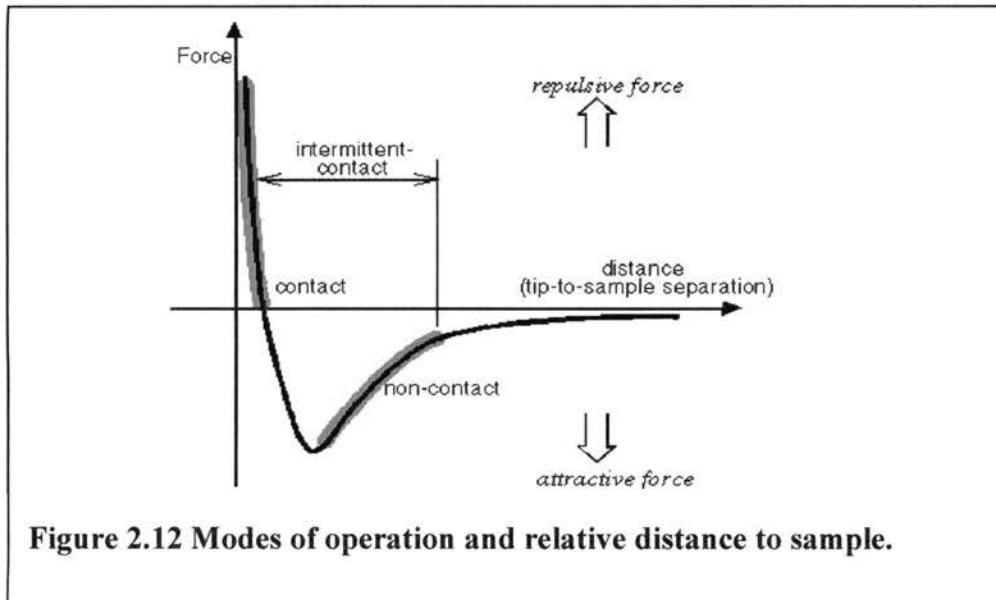
over the sample surface. It is this concept on which the basis of Atomic Force Microscopy is built.

2.5 Modes of Imaging and Related Forces

The theory has been presented that describes how there exists a range of forces at work on the AFM tip, depending on its separation from the sample. It should also be noted that the sample itself experiences forces; similarly to the tip, the surface is exposed to forces due to the van der Waal's, meniscus, and electron cloud forces. Because of this, many experiments are designed with the intention that the lowest possible force be exerted on the sample (while other experiments require a high force be used). This is of particular concern for very soft samples, such as imaging delicate crystal structures or biological samples.

The most common mode of operation for the atomic force microscope is called contact mode, which brings the tip very close to the sample surface and measures the repulsive force between outer molecules. This repulsive force data is then used to represent topographical information. Because this type of scanning exerts a relatively strong force on the sample by the tip, an alternate method of scanning at lower forces was designed. This type of scanning is called Non-Contact mode imaging, and positions the tip further from the surface. Because of its position, the tip in this mode monitors the attractive van der Waal's forces in the system. Since these forces are also distance dependent, it can be inferred that monitoring the van der Waal's forces can also provide information about surface topography. There is also a third mode of imaging, called Intermittent Contact Mode, which combines elements from both Contact and Non-

Contact Mode. Each of these three types of imaging has different applications, and a graph depicting the modes and the relative distances at which they are used is shown below:



The graph on the above shows that as a tip approaches the sample (moves from right to left on the graph), it initially feels a strong attractive force, due to the van der Waal's and meniscus forces. Then as it gets very near the sample (about 2-3 Angstroms), the repulsive forces due to electron cloud interactions begin to cancel out the attractive forces, until finally the repulsive forces dominate. The darkened regions labeled "Contact, Non-Contact, and Intermittent Contact" indicate approximate relative distance and force regions in which these modes operate.

2.5.1 Contact Mode

The most common mode of imaging is called "contact mode," and is named as such because it is in this mode that the tip and sample remain close enough to each other for the electron clouds of their outer most atoms to interact. This mode is chosen

generally for hard surfaces that do not damage easily, and sometimes for when slight surface distortion is desired.

In the contact mode of imaging, a “setpoint force” is chosen, which is the desired force to be maintained between the tip and the sample (usually on the order of nanoNewtons). As the tip approaches, there is an attractive force between the tip and the sample due to the van der Waal’s and capillary forces. Then, when the tip is within a few Angstroms of the sample surface, the tip experiences a repulsive force due to electron cloud interactions. The electronics then retract the tip away from the sample surface and comes to equilibrium at the setpoint force.

After the tip is in range, a scan can be taken using the general techniques described in the previous sections . As the scanner moves over the surface, the cantilever is deflected away from the sample by the repulsive forces between the tip and the sample. The laser light deflects onto a different portion of the photodiode detector, and this value in turn is used by the feedback electronics to adjust the position of the sample to maintain the setpoint force. The amount that the piezoelectric sample holder is moved is recorded as a topographical data point. The scanner then traces back and forth over the surface in a square area until an image containing 256 x 256 data points is obtained.

It should also be noted that the above process describes using contact imaging in the “constant force” mode, which is the more popular method of imaging. There is another method, called “constant height” imaging in which the feedback electronics are turned off, and the A-B signal is directly converted to a distance in which to map the topography (as opposed to the piezoelectric mount motion being used). This method is

less useful in many cases, particularly when the surface topography has a high range of vertical features. If the topography is too rough, the laser spot may be deflected out of the range of the photodiode detector. The constant force mode is often superior to constant height mode in that in-between each data point, the laser spot is repositioned near the center of the detector.

Although reasonably low set point forces can be chosen in this mode, it is sometimes the case that the close proximity (contact) of the tip can cause damage to the sample. This is of particular concern when studying biological samples such as DNA, proteins, or living cells. This problem can in part be addressed by imaging the sample in liquid or vacuum (if possible). However, to tackle this problem for biological and other soft sample studies, an alternative method of imaging was designed.

2.5.2 Non – Contact Mode

The non-contact mode of imaging is often used to image soft samples that are at risk of being damaged when scanned with contact imaging methods. This type of imaging keeps the cantilever tip and sample further apart, usually at a distance of tens to hundreds of Angstroms. Because of the greater distance in separation, in this mode the meniscus force usually is not a factor governing the setpoint force chosen for the experiment. The main forces at work are thus the van der Waal's force, and under some conditions, electric and magnetic forces.

The fundamental principle that enables this mode of imaging to work is that the cantilever chip that the scanning tip is attached to has a resonance frequency, much like a spring. This resonance frequency is dependent on the type, size, and material from which the cantilever is made. There are a variety of different cantilevers manufactured

commercially, from which a proper one can be selected for the experiment. It should be noted that if the cantilever is vibrated *at* its resonance frequency, then the cantilever will obtain its maximum vibration amplitude.

To prepare for taking a scan in non-contact mode, a fixed frequency is chosen that is near, but slightly higher than, the cantilever resonance frequency. The computer then sends a voltage signal to a piezoelectric material mounted on the non-contact cantilever holder. The piezoelectric vibrates the cantilever from the oscillating voltage in a similar way that the piezoelectric tube on the sample holder levels the sample surface.

The resonance frequency, ω , of the cantilever can be expressed by the equation,

$$\omega = (1/2\pi) * (k_{\text{eff}}/m)^{1/2},$$

where k_{eff} is the effective spring constant of the system, and m is the mass. When the cantilever is not in range of the sample (no outside forces affecting the system), k_{eff} is simply k , the spring constant associated with the cantilever itself. However, in the presence of outside forces (while in range, such as the van der Waal's force), k_{eff} is altered. The amount that k_{eff} is altered can be given by the equation,

$$k_{\text{eff}} = k - \partial F / \partial z,$$

where F is the spatial force affecting the system. It can be seen from this equation that F is dependant on the distance between the tip and the sample, and thus as the sample moves beneath the tip, the change in k_{eff} reflects surface topography. When this

information is substituted into the first equation, it is shown that changes in the force gradient (due to topography) affect the frequency of the vibrating system. The cantilever, altered in frequency, will thus have a different amplitude of vibration, and this property is used to interpret topography.

A feedback mechanism is also employed in this mode of imaging. After each data point is taken, the feedback mechanism acts on the piezoelectric material mounted on the cantilever holder to keep the selected frequency of vibration constant. The tip moves over the surface in the regular scan pattern, and the laser and photodiode detector are used to record changes in the amplitude of vibration of the oscillating tip. These 256 x 256 data points are recorded as topography.

Because of the small forces involved, this method of imaging has advantages over the contact mode for many types of samples. One major drawback of using this technique in air, however, is that because the tip and sample are further apart, and the system measures simply the magnitude of force between the two, contaminants such as the ever present condensation layer may distort topographical mappings. To try and address this issue, a third method of imaging, called Intermittent Contact Mode, was designed.

2.5.3 Intermittent Contact Mode

Intermittent Contact Imaging is similar to Non-Contact Imaging, however, as the name implies, the vibrating tip comes into contact with the sample intermittently. The cantilever is again driven at an oscillating frequency. However in this mode the tip is driven at a frequency slightly *lower* than the resonance frequency for the system. The reasoning of this can be understood by recalling that the cantilever will achieve its

maximum vibration amplitude when it is oscillated *at* its resonance frequency. When the tip frequency is slightly lower than this, and the cantilever (spring) is subjected to a downward force (due to van der Waal's), this force serves to increase the frequency of oscillation of the tip. Since the chosen frequency was lower than the resonance frequency, the theory is that the increase in frequency will in turn allow the cantilever to achieve a higher amplitude of vibration. Thus, as the tip traces over the surface, it comes into contact with the sample at the lowest part of its vibration.

As in Non-Contact Mode, the feedback electronics work to reset this system in between each data point, and the amount of change in the vibration amplitude of the cantilever is translated by the software to provide a map of the surface topography. Although more complicated and difficult to achieve, this mode of imaging has advantages over both Contact and Non-Contact modes of imaging. A lower setpoint force can be maintained, making this mode of imaging less damaging to softer samples. Also, besides penetrating the condensation layer hindering Non-Contact imaging, this mode of imaging has experimentally been proved to have a greater vertical range for scanning very rough or stepped samples¹⁴.

2.5.4 Other Methods

It should be noted briefly that while the aforementioned modes of imaging are commonly used to create mappings of surface topography, the AFM can be operated in a variety of ways to obtain an expanded description of the sample surface. One such operating mode is called Lateral Force Microscopy, or LFM, and can be used to measure not only vertical but also lateral forces exerted on the cantilever by the sample surface. This mode works primarily by dividing the photodiode detector into four quadrants

(instead of the normal two) so that the “twisting” of the cantilever can be more accurately recorded. In this way the LFM can produce not only a topographical image, but also can provide a mapping that indicates frictional variations (material dependant) on the sample surface.

Other methods of imaging include Force Modulation Microscopy (FMM), Magnetic Force Microscopy (MFM), Electrostatic Force Microscopy (EFM), and Scanning Capacitance Microscopy (SCM). When the AFM is operated in Force Modulation mode, the AFM tip is scanned over the surface in contact mode, while a periodic signal is applied to either the tip or the sample. The z feedback loop is used to keep the deflection of the cantilever constant in a manner similar to the method of constant force mode described above. It is in this way that elastic properties of the sample surface can be mapped, as the photodiode detector records deviations in the amplitude of the cantilever vibrations due to changes in elasticity in the material. When the AFM is operated in Magnetic Force Mode, the scanning tip is coated with a thin ferromagnetic material and the machine is operated in non-contact mode. When the coated tip is used to scan magnetic materials, a mapping of domain structures in the material can be made as the photodiode detector records changes in the resonant frequency of the cantilever induced by the magnetic field’s dependence on tip to sample separation¹⁵. It should be noted that in this mode, the separation between the tip and sample is slightly higher than in regular non-contact mode, to help distinguish topographical (van der Waal’s) features from the magnetic features due to the (farther reaching) magnetic forces.

Electrostatic Force Microscopy can be used to map locally charged domains on the sample surface by applying a voltage between the tip and (conductive) sample as the tip is moved above (and not touching) the sample surface. A mapping is made by measuring the magnitude of cantilever deflection due to changes in charge density on the surface. A potential difference between the tip and sample is also applied in Scanning Capacitance Microscopy, however the machine in this case is operated in contact mode. This mode is particularly useful in measuring capacitance properties important in the semiconductor industry, such as changes in dielectric material thickness, or dopant profiles in ion-implanted semiconductors¹⁵. Lastly, it should be noted that besides the five methods briefly described in this section, there are also several other modes in which the Atomic Force Microscope can be used to record a variety of properties describing sample surfaces. This versatility is part of what makes the AFM an invaluable tool in studying material sciences.

2.6 Calibration

As with many measurement devices, the Atomic Force Microscope must occasionally be checked, or calibrated, to ensure accuracy in its measurements of both distance and proportion. Over time the images may show some distortion or deviation from the true surface topography, and this is mainly due to properties inherent to the piezoelectric material on which the sample surface is mounted.

As has been mentioned, the main function of the piezoelectric tube beneath the sample holder is to ensure that the sample and the tip are maintained at a consistent level and distance (or force) apart. This is done when the feedback loop takes the deviation

signal from the photodiode detector and uses it to determine a voltage array to send to sections of the piezoelectric tube. This causes the tube to adjust the sample to return conditions to the setpoint force, and the vertical displacement of the tube is interpreted as reflecting topography. During this process, the software accesses a stored value for the ratio of distance versus displacement for the piezoelectric tube. Because of physical properties of the piezoelectric material, this value must be tested and adjusted on a fairly routine basis.

Two of the main piezoelectric properties that cause scanner non-linearity and the loss of proper calibration over time are called hysteresis and aging. As the piezoelectric material extends, retracts or shifts, it does not apply the voltage to distance ratio to its motion in a strictly linear fashion. In addition, when the material returns to its original position, the ratio is applied at a slightly different rate. Thus the scanner may require more voltage to retract instead of extending the same amount of distance. A graph depicting voltage applied versus displacement would show a deviation between mappings of extension and retraction. It is in this way that the tube seems to exhibit some “memory” over time, and the result is that an extended sample, when retracted, may not fully return to its original position.

Another property of the piezoelectric material that makes calibration necessary is related to its polycrystalline structure, and is called aging. Each crystal in the structure has a dipole moment, and the amount that the material can be displaced for a given voltage is dependent on whether the dipole moments in the crystals are aligned generally in the same direction. Regular use of the scanner helps maintain this alignment, however when the material is left unused for periods of time, the dipole orientations become more

random. What this amounts to is that over time, a given voltage may not move the piezoelectric material the expected distance, as fewer dipoles are in the proper position to assist scanner deflection.

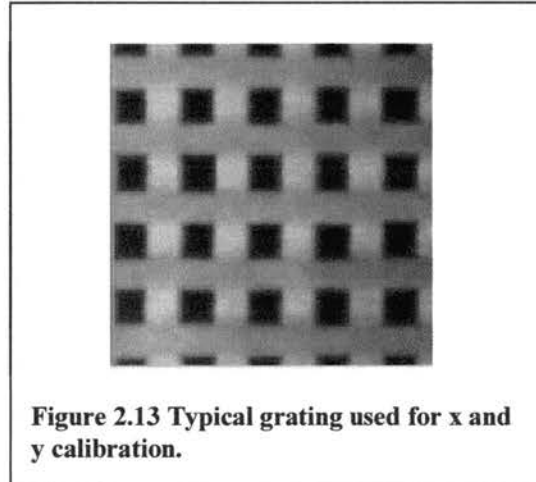
Because of these and other time and use related inconsistencies in scanning, a regular procedure must be employed by which the scanner is returned to accurate imaging capabilities. The best method to do this is to scan surfaces of known dimensions that can be compared with measured data. By using this data and simple ratio techniques, the stored values for voltage to displacement ratios can be adjusted to be consistent with actual conditions. This process can be done for both the horizontal (x and y) and vertical (z) directions.

2.6.1 X and Y Calibration

There are several methods by which horizontal calibrations can be made. All involving comparing data values from a known structure with results of surface analysis with the microscope. One common method that calibrates both the x and y direction simultaneously is to scan a cleave of graphite, which has a regular hexagonal crystal structure. The software can be used to create a fast Fourier transform of the scan, which will provide a general representation of the overall structure of the lattice units. The angles between atoms of this crystal structure are well defined, and this value is compared with the fft image. The voltage to distance value is then adjusted by means of a simple ratio.

An easier and more common way to calibrate the AFM is done by employing commercially designed structures, in the form of tiny square (screenlike) gratings. There are two gratings used in the laboratory, one each for the five and hundred micron

scanners. The small and large gratings have periodicity of 1.0 and 9.9 microns, respectively, in both the x and y directions. An example of this type of grating is shown below:



The first step in the calibration process is to obtain a good scan, at a scan size large enough to encompass several periods of the grating. The axes of the grating must also be properly aligned with the axes of the scanner, which may require repeated minute adjustments of the scan head. This is important because a line scan (single line of data) is required on which to make periodicity measurements, and an improperly aligned grating would produce distorted line scan results.

After a scan of sufficient size and alignment is made, imaging processing software on the AFM computer allows measurements to be taken in specific directions on the grating scan. The software enables the user to select a single line of data in the x direction, and provides a distance measurement for a specified number of periods. From this an average period length is determined. This method is used because average length provides more accurate data than if a single period measurement is used. By comparing

this value with the known value, a ratio can be used to adjust the voltage to distance value.

The process works like this: suppose the 100-micron scan head is used to image a calibration grating with a periodicity of 9.9 microns. The image is then loaded into the data analysis software, and a line scan in the x-direction reveals that four periods of the grating appear to be 41.2 microns instead of the expected 39.6 microns. The user would then open the calibration file appropriate for the scan head, which in this case is located at c:\psi\cal\100 μ m.scn. In this permanent file, a numerical factor is stored which represents a voltage to distance ratio for the x-direction. The AFM software refers to this file when voltage readings from the photodiode detector are translated into an image representing topography. The line of data containing this factor looks like this:

$$\text{MicronPerDac_Sx/Hi.sps} = 2.7017.$$

To calibrate the software, the user would then adjust this numerical factor by a ratio of the known value of the grating to the imaged value. In this case, the ratio of adjustment would be 39.6/41.2, or 0.961. The new conversion factor line would then read:

$$\text{MicronPerDac_Sx/Hi.sps} = 2.5968.$$

This process is then repeated to calibrate in the y-direction. After the values for distance to voltage ratios are adjusted, it is useful to shut down the AFM software system and reboot. Another scan of the calibration grating should be taken after rebooting, and if necessary, the ratio process can be repeated.

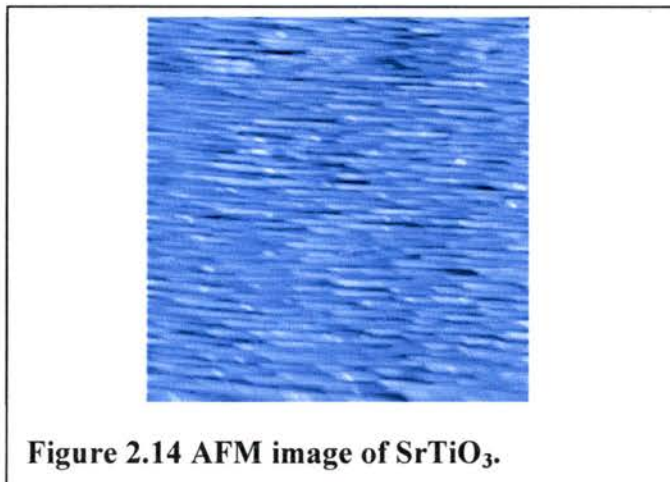
2.6.2 Z Calibration

Vertical calibration of the AFM system is also very important, because the fundamental technique of the imaging system is to provide height information of points at

regular intervals. This is also very important when using the AFM to provide information on film thicknesses, feature height or grain size. As with horizontal calibration, there are both Cartesian and angular calibration techniques.

The more straightforward method of z calibration is to scan a surface of known step height, and there also exist commercial products manufactured specifically for this purpose. The voltage to distance ratio saved in the software files are adjusted in the same manner as described for the x- and y-calibrations.

Another way to calibrate the vertical range of the AFM scanner is to use a both a vertical and angular approach. In this approach the AFM is used to scan a material with a known crystal structure, such as SrTiO_3 . The material is cut so that well-defined terraces protrude from the surface at regular angles, due to the crystalline nature of the material. When this type of sample is imaged and then loaded into the data analysis software, a line scan will reveal the software's interpretation of the crystalline angle. If this angle is not concurrent with the known value for the structure, the calibration file for the scan head can be adjusted in a ratio manner similar to the one described previously. This method of vertical calibration is superior to the more direct approach, in that angular factors of calibration, due to things such as piezoelectric tube aging, can be corrected.



2.7 The Microcell

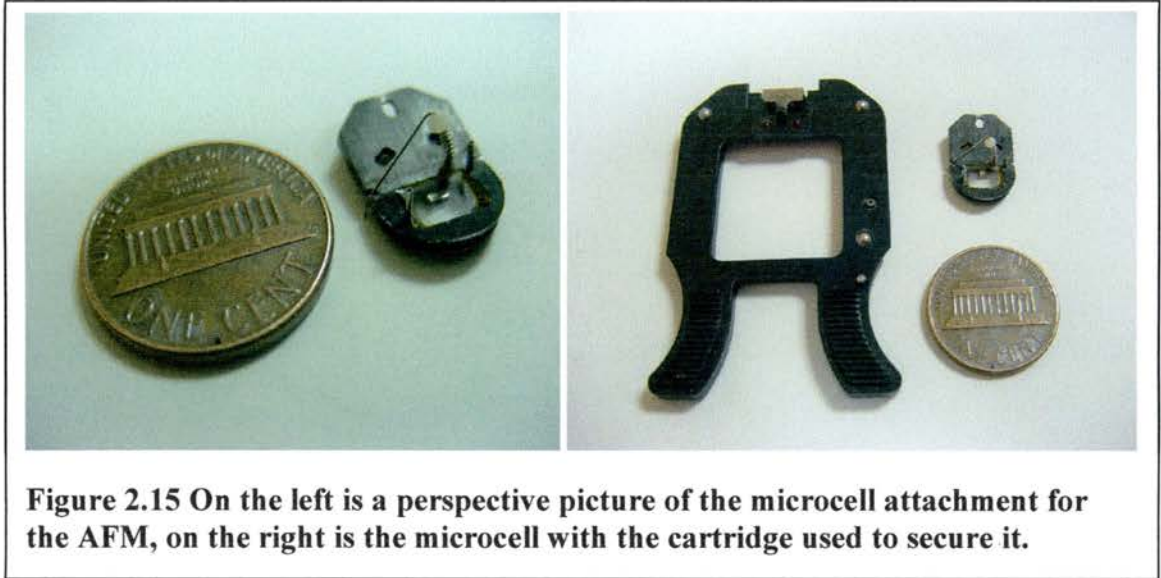


Figure 2.15 On the left is a perspective picture of the microcell attachment for the AFM, on the right is the microcell with the cartridge used to secure it.

The picture above shows an attachment for the AFM called a microcell that allows images to be taken while the sample is exposed to a liquid solution (called *in situ* imaging). The cantilever is secured inside the glass-topped chamber by means of a spring-loaded clamp, and the entire component is secured to the contact mode cantilever holder cartridge in a manner similar to that of the regular cantilever holder. Solutions are either injected or dropped into the liquid chamber with a small syringe, and the glass window on the top of the microcell allows the AFM laser light to pass through and be focused on the back of the cantilever. Because of the additional mediums that the light must pass through (the glass and the liquid), focusing of the laser is slightly more difficult with the microcell and will be discussed in more detail in section 3.3.1.

One common application of using the microcell with atomic force microscopy is to study the effects of exposing metals to corrosive solutions. The microcell makes it

possible to see a step by step progression of the process, and the imaging software for the AFM enables researchers to study properties of the metals such as grain structure or roughness during the corrosion sequence. An added benefit to using the microcell is that because the tip-sample system is completely immersed in liquid, the meniscus force described section 2.4 is eliminated, allowing imaging to be done at very low (non-damaging) forces.

For this project, the microcell proved particularly useful for studying the mechanisms of CMP, in that it was used to help model the effect of a single abrasive particle acting on a surface while exposed to a corrosive solution. The microcell was filled with the same solution (minus the abrasive particles) that was in the polishing slurry used to smooth copper in the polisher. The cantilever tip tracing across the sample surface at a set force represented a single abrasive particle being pressed against a sample by the polishing pad.

CHAPTER THREE

EXPERIMENTAL PROJECTS

3.1 Experiment Design

One of the first projects involved with designing an experiment to examine the processes involved with CMP was to choose what type of polishing solution to use. The polishing slurry used in the polisher normally consists of three components: a corrosive solution, a corrosion inhibitor, and the abrasive particles. Some early experiments were done using the AFM to try and determine what types of solutions in what concentrations would be useful towards studying the CMP process.

3.1.1 Corrosion Inhibitor

A corrosion inhibitor is used in the planarization process to help control the amount of time a given area is exposed to a corrosive solution. A corrosion inhibitor is thought to work in the following manner: as a material to be polished is exposed to the slurry, a thin layer of the corrosion inhibitor coats the surface. This layer acts to protect the material from the corrosive component of the solution. Then, as an abrasive particle is brushed across the surface by the polishing pad, the particle temporarily pushes the corrosion inhibitor away from the material. In this short time interval, the surface is now exposed and the corrosive chemical has a chance to act upon the material until the corrosion inhibitor resettles over the surface. This process aids in smoothing the surface because the abrasive particle is more likely to remove the inhibitor on raised portions of

the surface. Thus by repeating this process, the surface becomes more planar and smooth.

Without this corrosion inhibitor, the corrosive solution will act upon the entire surface continuously. This will result in an increase in material removal, however also in a decrease of surface planarization. A chart below shows how the RMS roughness of two samples differ when a piece of silicon coated with copper was polished with a nitric acid solution both with and without a corrosion inhibitor called benzotriazole (BTA):

Sample	10 micron scan	30 micron scan	80 micron scan
# 1, with BTA	38.5	58.6	67.3
# 2, with BTA	29.4	54.8	70.2
# 3, with BTA	21.7	51.1	74.3
# 4, no BTA	437	787	804
# 5, no BTA	374	816	960
# 6, no BTA	248	845	1100

Table 3.1 This chart displays the RMS roughness, in Angstroms, of 6 copper samples that were polished and then analyzed at sizes of 10, 30 and 80 square microns.

As can be seen from the chart, the samples polished without the corrosion inhibitor were much rougher than those polished with benzotriazole. Because the goal of CMP is to produce a very smooth surface, the decision was made to include BTA in both the polisher and AFM trials.

3.1.2 Corrosive Solutions

Two corrosive solutions that are commonly used in the CMP process are nitric acid (HNO_3) and ammonium hydroxide (NH_4OH). Some preliminary testing was done using these solutions to try and determine what concentrations would be useful in the

AFM experiment. It was not feasible chemically to combine ammonium hydroxide and the available corrosion inhibitor (BTA), thus nitric acid was chosen for testing. It was desirable to choose a solution strength that would have a measurable effect on the copper, however worked slowly enough to be used in a controlled manner. The AFM was used to make roughness measurements on samples exposed to the solutions for varying amounts of time. Solutions of ammonium hydroxide (and water) and nitric acid (and water) were prepared in Molar concentrations of 0.02, 0.035, 0.05 and 0.065. Most of the samples showed no significant change in RMS roughness after being exposed to the 0.02, 0.035 and 0.05 solutions, but a measurable (about 12%) increase in roughness was observed for samples exposed to the 0.065 M nitric acid solution. Because this change was small yet observable, the 0.065 M nitric acid solution was chosen for the AFM experiment.

3.1.3 Abrasive Particles

The slurry used for CMP contains tiny abrasive particles, most commonly made of aluminum oxide, that are available in a variety of sizes. In the polishing process, these particles can be used singularly, or in succession, much like using sandpaper in a progression from coarse to very fine. In the lab, aluminum oxide particles are available in three sizes with average diameters of $0.3\mu\text{m}$, $0.1\mu\text{m}$, and $0.05\mu\text{m}$. Since one of the goals of this experiment was to closely model the polishing process with an AFM tip, the smallest available particle selection was used to polish the copper films. This is because the $0.05\mu\text{m}$ (50nm) size most closely relates to the size of the AFM tip.

3.1.4 Varying pH

The primary variable explored in the CMP-AFM experiment was the relationship that the pH of the polishing solution had with the smoothness of the copper samples after they had been processed. This variable was chosen because a related study done on tungsten surfaces by Lim et al²² had shown that the pH of solutions used in the microcell have a measurable effect on the amount of friction observed between an AFM tip and sample. Since initial testing had shown that 0.65M Nitric Acid was a useful solution to use in the trials, this solution was buffered with either acetate (pH 4) or phosphate (pH2 and pH6) buffers to create solutions of pH 2, pH 4, and pH 6. A solution of pH 7 is neutral; so these buffered solutions are considered very acidic, acidic, and slightly acidic, respectively. These solutions were used in both the polisher and also in the AFM microcell trials. In the microcell, a solution of deionized water was used as a control to ensure that .

3.1.5 *Ex Situ* vs. *In Situ*

Another main goal of this experiment was to explore whether the AFM microcell could be used to model the CMP process. The AFM was used in two ways; first to examine copper thin films after they had been polished (*ex situ* studies), and secondly to use the AFM microcell itself to directly imitate the polishing process (*in situ* studies). It was hypothesized that analyzing images using these two techniques would provide comparable data. Because of slight variations in the polishing environments (to be discussed more fully in the following sections), it was theorized that although these analyses might not be directly comparable, they both might show similar trends relating pH level to surface planarity.

3.2 *Ex Situ* Studies

The goal of this portion of the experiment was to use the atomic force microscope to measure properties of copper thin films that have been polished using a Buehler metallographic polisher. The pH of the polishing slurry was varied between trials, while keeping the other polishing variables (such as exposure time, rotation rate, and particle size) constant. The AFM was then used to profile the samples, using the RMS roughness of the samples as an indication of planarization.

3.2.1 Procedure

Small (about one 1.5 cm by 1.5 cm) samples were cut from a large silicon wafer coated with a thin copper film. Each of these were laid at the bottom of a rubber mold, which was then filled with epoxy and cured to create a small cylindrical sample holder that could be mounted in the polisher. The samples were then polished for five minutes each, at varying solutions of pH 2, pH 4, and pH 6. The sizes of the polishing particles were consistent between trials, having an average diameter of 0.05 microns. To study polishing consistency, three samples were prepared for each pH level.

After the polishing step was completed, the samples were rinsed and prepared for the AFM. Since the samples were firmly bound to epoxy mounts, much of the excess epoxy was removed with a metal file and the bottom of the epoxy mount was leveled. The samples were then attached to magnetic sample holders and loaded onto the AFM stage. Several scans were taken of varying sizes with both the five and hundred micron scan heads, in contact mode. Scans were also taken of “as received” copper films for comparison. The results of this analysis are described in the following section.

3.2.2 Data

Data charts and graphs depicting the data taken during this portion of the experiment are given on the following pages. The first two pages of graphs represent data taken with the higher resolution scan head, with images taken at sizes of 1, 3, and 5 microns square. The second two pages of data were obtained with the lower resolution scanner, at scan sizes of 10, 30, and 80 microns square. Several scan sizes of each pH level were taken in order to explore which scan sizes were appropriate for the experiment.

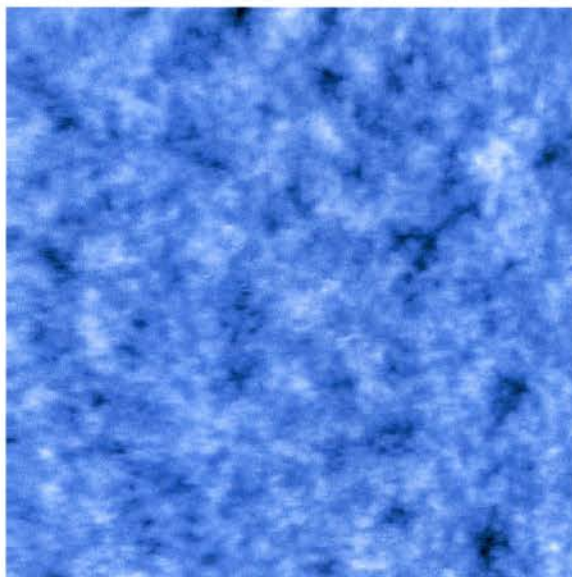
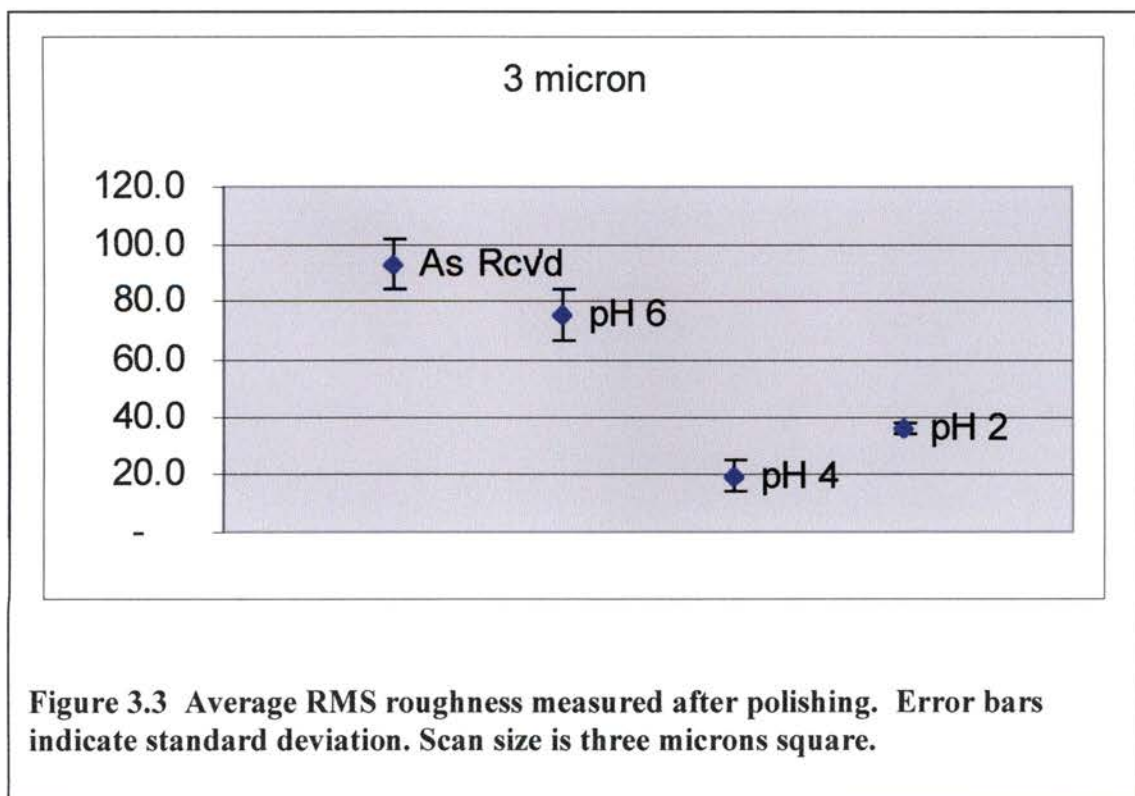
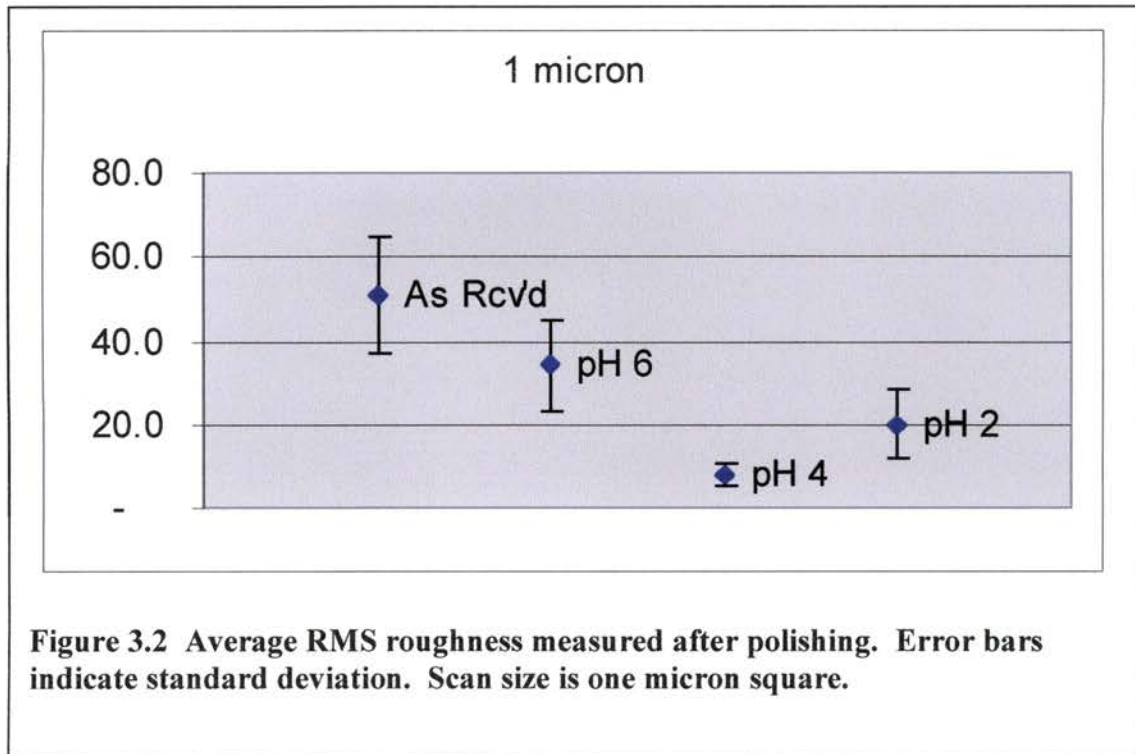
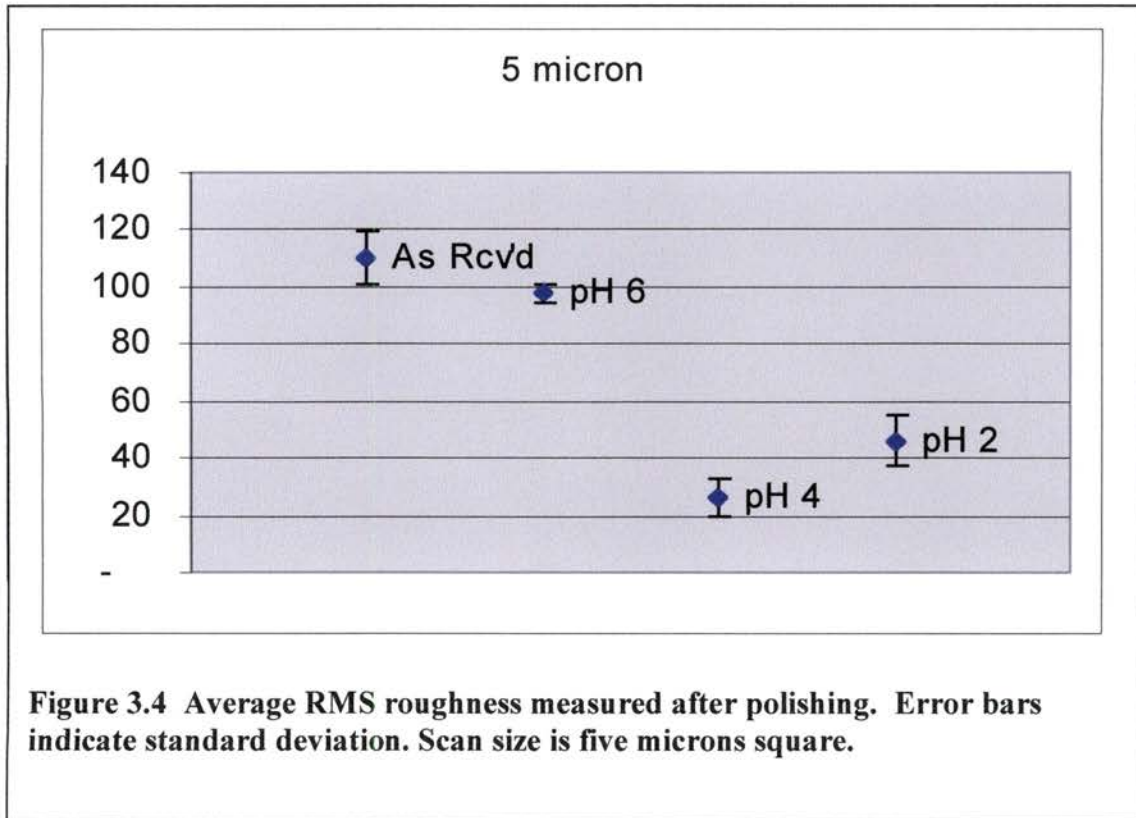


Figure 3.1 An example of a copper scan; this particular picture is a 30 micron scan of “as received” copper.

EX SITU SMALL SCALE DATA				
	1 micron	3 micron	5 micron	
	67.0	88.7	121	
As Received	41.2	87.0	103	
	44.7	103	106	
	51.0	92.9	110	
	10.4	33.7	35.7	
pH 2	25.8	36.8	51.0	
	23.6	37.5	50.9	
	19.9	36.0	45.9	
	8.07	24.9	33.3	
pH 4	5.15	13.5	23.5	
	10.6	19.2	20.8	
	7.94	19.2	25.9	
	36.9	65.5	94.4	
pH 6	21.9	82.8	97.2	
	43.5	77.0	101	
	34.1	75.1	97.5	

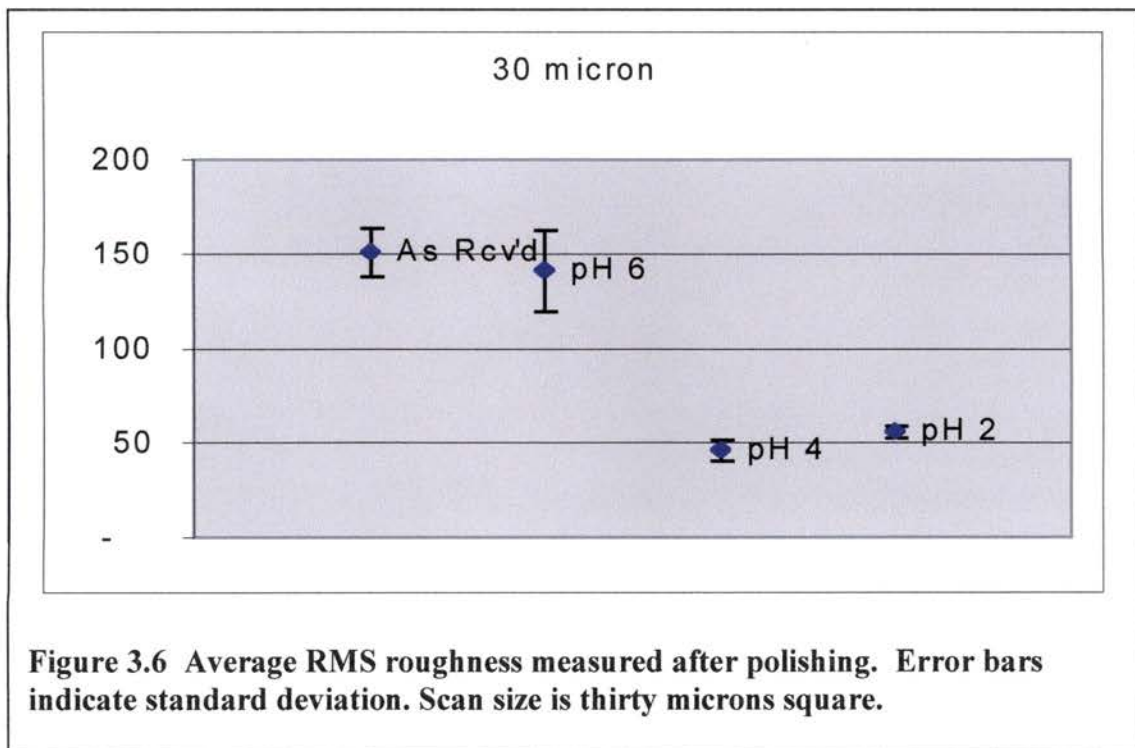
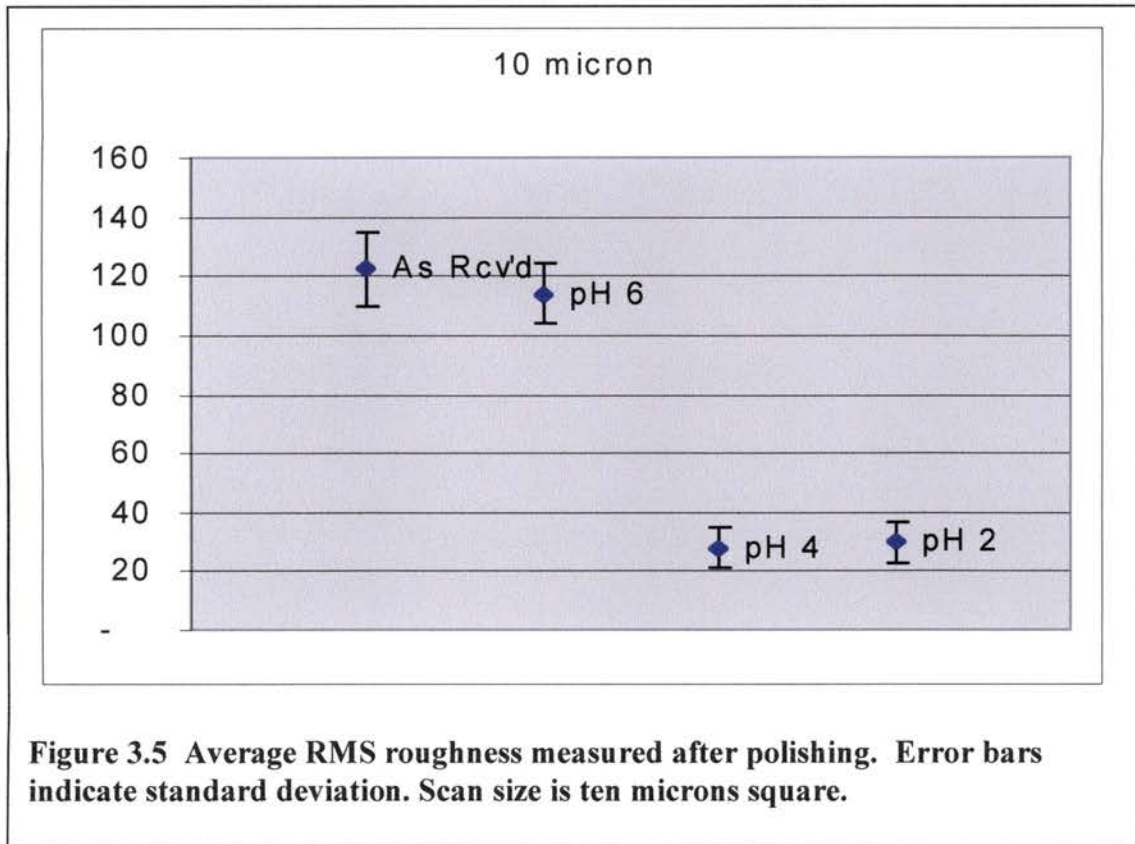
Table 3.2 RMS roughness, in Angstroms, of samples examined ex situ after being polished with solutions buffered to pH 2, pH4, and pH6. Averages are shown in red.

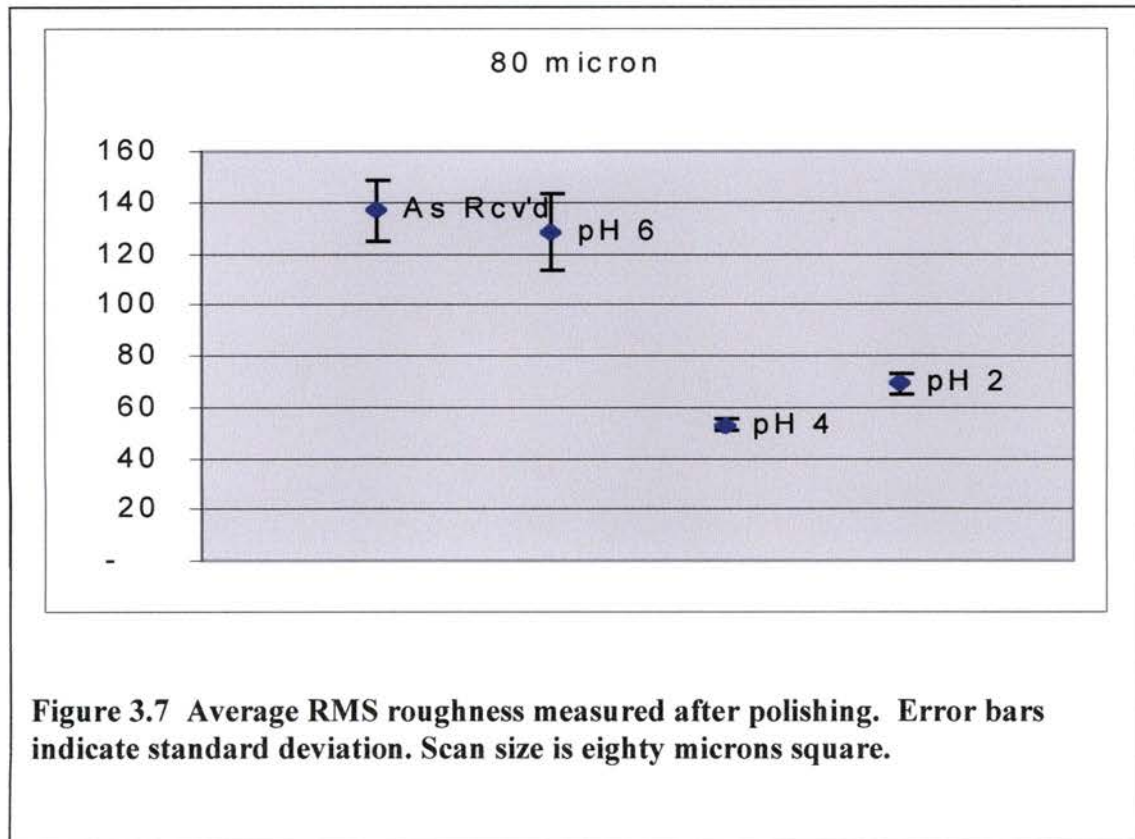




EX SITU LARGE SCALE DATA			
	10 micron	30 micron	80 micron
	136	171	152
As Received	124	146	137
	106	142	122
	123	145	136
	122	151	137
	38.5	58.6	67.3
pH 2	29.4	54.8	70.2
	29.5	57.4	64.3
	21.7	51.1	74.3
	29.8	55.5	69.0
	23.0	40.1	52.1
pH 4	21.7	41.4	54.0
	34.9	48.4	50.2
	32.4	52.0	55.4
	28.0	45.5	52.9
	120	168	141
pH 6	121	123	111
	116	124	121
	99	150	140
	114	141	128

Table 3.3 RMS roughness, in Angstroms, of samples examined ex situ after being polished with solutions buffered to pH 2, pH4, and pH6. Averages are shown in red.





3.2.3 Discussion

There are several observations that can be made about the data obtained by analyzing the polished copper *ex situ*. To begin with, the uniformity between scan sizes suggests that all of the scans taken are in an appropriate range to study the effects of CMP polishing. The fact that a similar trend can be observed at both 1 and 100 micron scan sizes suggests that the grain size of the copper film is not too large to interfere with 1 micron scan analysis.

Perhaps the most important result of these trials is the marked dependence, in every case, of the planarity of the surface with the pH of the solution used in polishing. As can be seen, the solution of pH 6 showed the least amount of planarization (compared with “as received” films), while both the pH 2 and pH 4 showed a significant improvement in smoothness.

Another interesting result of this experiment was that the copper films polished with solutions of pH 4 were slightly more smooth than those polished at pH 2. This implies that the relationship between planarity and pH level is not monotonic. This may be due in part to effects that the pH level may have on the friction between the polishing particulates and the sample. In a recent study related to this experiment done by Min Soo Lim and Scott Perry, it was shown that the friction between an *in situ* tip of an Atomic Force Microscope and a tungsten sample varied with the pH of the liquid in the AFM²². This dependence was not of a monotonic nature, but instead suggested an inverted “bell” shaped curve. The results of the *ex situ* experiment appear to suggest a similar trend, and

the similarity between the two experiments may indicate the dependence of friction on pH level may be a factor in planarizing copper.

3.3 *In Situ* Studies

The goal of this portion of the experiment was to use the microcell attachment for the AFM to simulate the effect of a single abrasive particle coming into contact with a copper film in the presence of nitric acid. As has been mentioned, some of the variables involved with the CMP process involve the pressure between the abrasive particle and the copper, the size of the abrasive particle, and the composition and concentration of the corrosive solution. For this portion of the experiment, the set point force was kept constant between trials, and the pH of the corrosive solution was varied. This was done in the same manner as the *ex situ* trials, with a total of four *in situ* trials: one trial in water and one trial in each of pH 2, pH4, and pH 6.

3.3.1 Procedure

Each of the *in situ* trials was done on a small cutting of “as received” copper film on a silicon substrate. The samples were prepared in the normal fashion, being mounted on magnetic samples and dusted with air. After loading the microcell with a fresh cantilever chip, the chamber of the cell was filled by syringe with either water (for the “as received” control trial) or polishing solution. This was done while the microcell was inverted, and once flipped the surface tension of the liquid kept the fluid in the chamber.

As with every scan, the laser had to be focused onto the back of the cantilever chip and the photodiode detector adjusted into position to capture the reflected beam. This step proved more difficult with the microcell than with the normal cantilever holder. The reason was that the laser light refracted (bent) twice before hitting the back of the

cantilever, once at the air-glass interface and a second time at the glass-solution interface. Snell's Law describes this effect. Also, a portion of the laser light was reflected rather than transmitted at each interface. This caused two problems. One was that the beam captured by the photodiode detector was less intense than it would have been if only passing through air. Because of this it was very important to precisely focus the laser and position the photodiode detector. Although the captured beam was generally less intense (a maximum A+B signal of about 1 Volt, instead of the usual 1.5 – 2 Volts), it was still possible to track the motion of the cantilever with this method. The other problem encountered was that more than one beam of light was reflected from the microcell system, one was the true beam from the back of the cantilever, and another bright beam reflected from the air-glass interface (also, a dim third beam emanated from the glass-solution interface). This problem proved more difficult to eliminate and was addressed by carefully positioning the cantilever cartridge so that the undesired beams were reflected onto the back wall of the machine and not into the path of the photodiode detector.

After focusing the laser and carefully monitoring the A+B and A-B signals of the photodiode detector, the scan head was carefully lowered by (a slow) manual approach onto the sample surface so that the liquid (and not the cantilever) came into contact with the surface. It should be noted that for this step it was sometimes helpful to put a small drop of solution onto the sample surface and lower the scan head until the surface drop and the suspended drop of solution from the microcell formed a meniscus. At this point the laser light must again be adjusted to compensate for the meniscus force now pulling

the cantilever towards the surface. After the voltmeter signals are properly adjusted, the head was then lowered by computerized approach.

After the tip is in range of the sample, the scan parameters such as slope, size and setpoint force were set. In this experiment the five-micron scan head was used to take one-micron scans at a setpoint force of 25 nanoNewtons. The scan software has can be set to automatically repeat the scanning process, and 20 scans of each sample were taken at a rate of 2 Hertz. Since the machine scanned across the sample and back in one second, each scan took a total of 256 seconds (or about 4.3 minutes) to finish. Therefore the total exposure time of each sample to the corrosive solution was about an hour and a half.

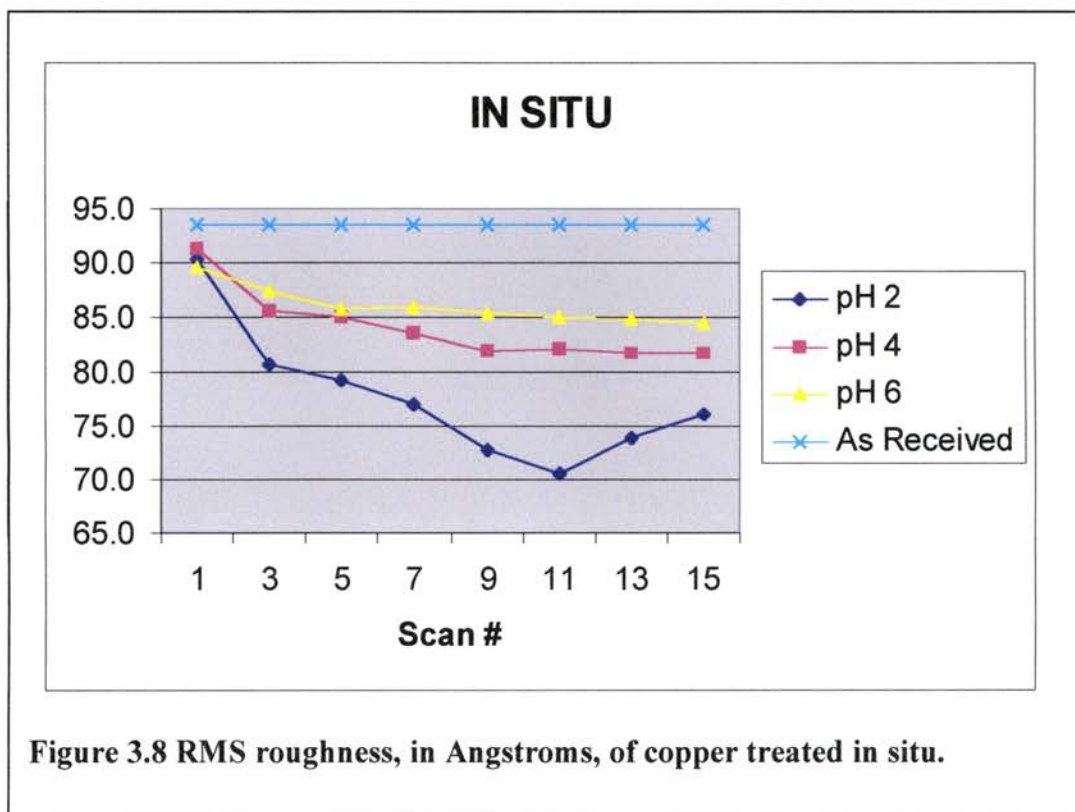
After completing this process, the 20 scans from each experiment were loaded into the computer image processing software and flattened. Flattening is a computer process that analyzes the data in three dimensions and then repositions the image so that it is as aligned as possible in the z-direction. This process is important in obtaining accurate image analysis so that distortions due to improper tip-sample alignment are filtered out. After this was done for all of the images, a selected portion of each image was analyzed for surface roughness. The results of this analysis are described in the next section.

3.3.2 Data

A data table and graph depicting the results of this experiment are given on the following page. It should be noted that although 16 scans of each pH sample were taken, there was a slight amount of drift as the scanner alternated between upward and downward scans. For this reason, the data shown reflects only upward scans.

IN SITU DATA TABLE				
scan no.	As Received	pH 6	pH 4	pH2
1	93.5	89.6	91.4	90.4
3	93.5	87.5	85.6	80.7
5	93.5	85.8	85.0	79.1
7	93.5	85.9	83.5	77.0
9	93.5	85.4	82.0	72.7
11	93.5	85.0	82.2	70.5
13	93.5	84.8	81.7	73.8
15	93.5	84.6	81.7	76.0

Table 3.4 RMS roughness, in Angstroms, of copper samples studied in situ with the microcell.



3.3.3 Discussion

One of the most promising results of the *in situ* experiment is that although the results may not be directly comparable with *ex situ* data, the microcell trials show a similar trend as the trials examining post-treatment copper. As can be seen by the graph on the preceding page, the two trials that used more acidic solutions (pH 2 and pH 4) were more successful at planarizing the surface, while the more neutral solution (pH 6) maintained a roughness value closer to that of the “as received” sample. One thing to note however, is that the *in situ* scans did not seem to exhibit a bell shaped dependence of pH with planarity that was suggested in the *ex situ* experiment. Since only one trial of each type was performed, a standard deviation of the data is not available. Applying a general error rule of thumb of 10% reveals that it may be shown during further testing (with improvements suggested in Chapter 4) that the positions of pH 2 and pH 4 are reversed. Theories concerning the discrepancies between *ex situ* and *in situ* experiments are discussed in Chapter 4.

One other interesting result of the microcell trials is that it can be seen that after about an hour of scanning (after scan number 12), the roughness of two of the samples actually increased. This is seen most clearly by looking at the scans for pH 2. There are several hypotheses for this behavior. One is that over time, the solution in the enclosed microcell becomes somewhat saturated with loose copper particles. In a full scale polishing system, this excess material is removed by a continuous rinsing of the sample surface, either with fresh slurry or water. Since this excess material was not removed in the microcell, it may be possible that some of the copper either settled or re-adhered to

the surface, causing the roughness level to rise once again. The fact that this effect was most marked in the most acidic solution seems to concur with this theory. The pH 2 may also have affected the solubility of copper and removed the most surface material, causing the solution to become more dense with copper particles.

A discussion of how the *ex situ* and *in situ* trials compare with each other is given in Chapter 4.

3.4 AFM tips

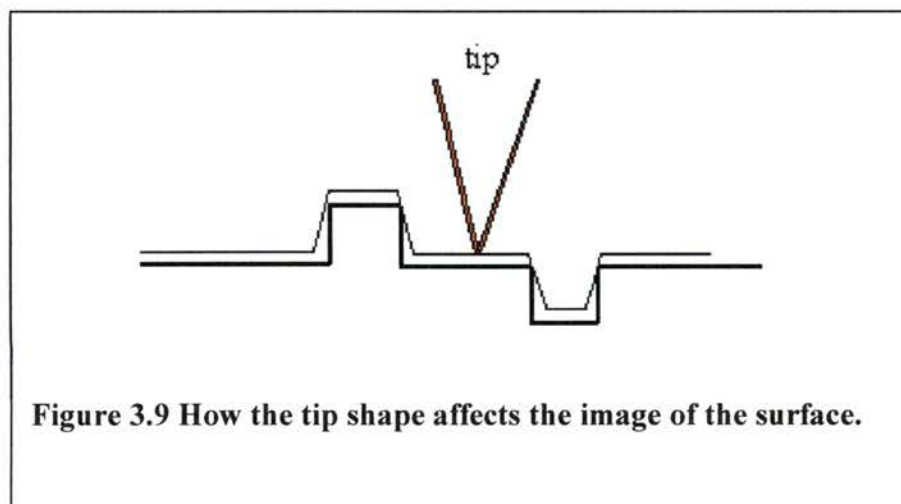
Since the surface features and forces involved with Atomic Force Microscopy are so small, it is clear that one of the most critical components of the AFM system is the scanning tip mounted on the cantilever chip. There are several different types of tips available, mounted on a variety of cantilever chips varying in size, material, and force constants.

The very first AFM tip was created by attaching a small piece of diamond (tip) to a thick piece of gold foil (cantilever)¹⁶. Today, cantilevers are microfabricated in large quantities and manufactured on wafers containing around 600 chips. They are typically made from either silicon (Si) or silicon nitride (Si₃N₄), and are coated with a highly reflective material (usually gold) on the side on which the AFM laser deflects.

The cantilever chips on which the tips are mounted come in a variety of sizes, and, more importantly, a variety of spring constants (k) and resonance frequencies (ω). The spring constants available are generally on the order of .001 to 100 N/m, and the spring constant of the cantilever used in the liquid cell experiments was approximately 0.26 N/m. The available resonance frequencies usually range from tens to hundreds of

kiloHertz, and the one chosen for this experiment has an ideal resonance frequency of 40 kHz. Having this range of choices available for cantilevers is important, and in particular can be seen in relation to the equations given in section 2.5.2. It can be seen by these equations that the spring constant and resonance frequency of a cantilever are related with the maintained setpoint force involved in scanning. By choosing the appropriate cantilever, scanning at very low forces can be achieved.

Besides properties of the cantilever chip, determination of the geometry of the scanning tip itself is very important to Atomic Force Microscopy. Since the features of many of the images are so small (on the order of nanometers), having an atomically “sharp” tip is critical. If the tip is too blunt or short, it may not be able to reach into many of the crevices in the sample. Ultimately, the images generated by the AFM are dependent on the forces between the tip and the sample, and these forces are determined not only on the topography of the sample, but also on the geometry of the tip itself.

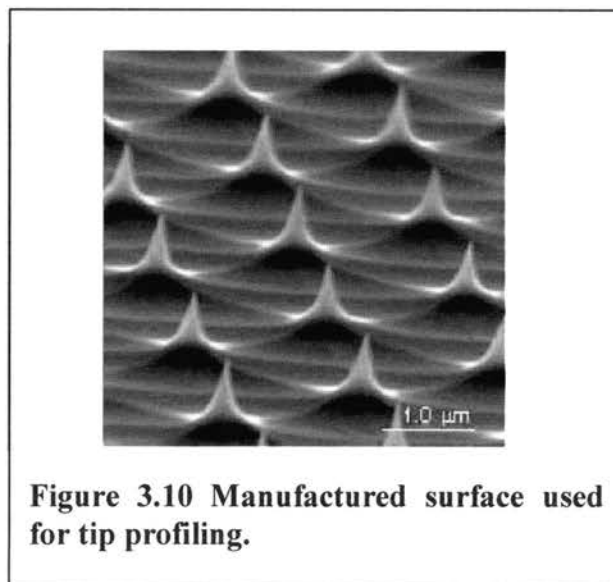


For example, an image with a rounded feature may not be the result of a sharp tip scanning a rounded surface, but rather a blunt tip interacting with a sharply angled

surface. Also, misshapen tips, such as a “double tip” with two or more protruding apexes, may produce images with artifacts or features that are not really there. This type of distortion is called “convolution.” Convolution is defined as the linear combination of two functions. In this case, the two functions involve the actual surface features (surface function), and the ability of the tip to accurately model the surface (machine function)¹⁷. It is for these reasons that having a method to profile AFM tips is critical to producing accurate, high-resolution images.

3.4.1 Tip Profiling

The primary method for profiling an AFM tip is to scan the tip over a known, regular surface, and to use a mathematical algorithm called “blind reconstruction”. Almost any semi-rough surface can be used for this type of scan, but a particularly useful type of sample is available commercially and pictured below:



This sample is made of silicon, and was chosen because of its sharp, regular peaks. The heights of the peaks are useful so that the sides of the tip can also be profiled. A scan

over this surface is taken, and then the image is loaded into a computer program that uses the blind reconstruction method.

Blind Reconstruction is a method by which the computer generates limits (both upper and lower) for the size and end radius of the AFM tip. The first step in this process is to examine a single bump (or peak, in the silicon profiler sample) scanned by the cantilever tip. By examining the geometry of this scan, two potential tip shapes can be hypothesized. The lower bound is determined by assuming that the image shape is fairly accurate in comparison with the actual sample geometry. The upper bound is determined by assuming that the tip is very blunt and scanning over a sharp object, however, it can be no more blunt than the actual scanned image itself. The computer then repeats this method for all of the features on the scan, and it should be noted that smaller (sharp) features are more useful for this technique. As the data from each of these features is compiled, an estimate for the actual tip structure is formed, in three dimensions. It should be noted that this estimate is actually an upper bound for what the tip may look like, when in reality it may be more sharp and defined.

This technique is useful for a number of reasons. One is that by knowing the approximate shape of the tip, the computer can then apply this tip shape to the image an attempt to produce a “deconvoluted image.” This technique “cleans up” an image, possibly removing artifacts and providing a more accurate model of the surface features. Deconvolution works by placing the approximated tip shape at each of the 2^{16} data points in the image. As it is applied to the point, the features nearby that data point are adjusted to better match the approximate tip shape. Thus the computer takes the tip’s geometry,

and the original image scan, and estimates what actual surface would produce the given image with that tip.

Another way that tip profiling can be useful relates to the CMP-liquid cell simulation. An important variable in chemical mechanical planarization is the size of the particulate dissolved in the polishing slurry. An analogy to this process would be using sandpaper, where larger grained sandpaper would be used for quickly removing excess material, and a smaller grain would be used for fine polishing. In CMP both material removal and fine polishing are factors, used in different proportions for different applications. Knowing the area of contact of the particle is important in determining the pressure exerted by the particle on the wafer. The pressure exerted by the particle is directly related to the force exerted by the polishing pad, and inversely proportional to the area of contact.

Thus it is fundamental to any meaningful comparison of *ex situ* and *in situ* polishing data in the liquid cell experiment to know the shape of the tip in question. In the case of the silicon Ultralever tips, some uniformity is expected because of the precise method in which these tips are manufactured. The ideal dimensions of these chips are given in their promotional materials, and the Ultralever tips used for the AFM experiment are advertised to have a radius of curvature of about 500 Angstroms (50 nm). However, to account for defects both from manufacturing and handling, it is in the interest of this experiment to attempt to profile the tips used in the liquid cell.

3.4.2 Coated Tips

Another project closely related with the CMP-AFM simulation is involved with coating the cantilever tips used for scanning with a material similar to one used in the

abrasive particles used in Chemical Mechanical Planarization. To do this, a process called sputtering was used, with a machine called the DC Magnetron.

Sputtering is a process by which a target (the material to be deposited) is bombarded with energetic ions¹⁸. In this case, the material chosen for deposition was aluminum oxide (Al_2O_3), since the particulates in the polishing slurry are made from alumina. The ions are introduced by flowing charged Argon gas into a vacuum chamber containing the aluminum target and a holder designed to firmly secure a set of ten cantilever chips. The chips are mounted into the holder upside-down, to expose the tiny tips to be coated and protect the reflective gold coating on the back of the chip. When the Argon gas enters the chamber, charged ions impact onto the surface of the aluminum target. A transfer of kinetic energy then knocks some of the aluminum atoms loose, and these are deposited onto the inside of the chamber (including onto the cantilever tips). The thickness of the film that is deposited can be adjusted by monitoring the rate of flow of the gas and the amount of time that the chips are exposed.

Both the thickness and structure of this film are of importance to the CMP-AFM project. One property of the film that was studied with the Atomic Force Microscope was the grain structure of the alumina layer that was deposited onto a flat substrate. Grains are tiny clusters of atoms that group together on both on the alumina coating and on the copper samples to be studied. If the alumina grains were too large, the coating may be too rough to use in the CMP simulation. The AFM was used to image a piece of silicon coated with a film of aluminum oxide, and a roughness analysis of the film showed that the film was only slightly rougher than the silicon alone. Since the alumina

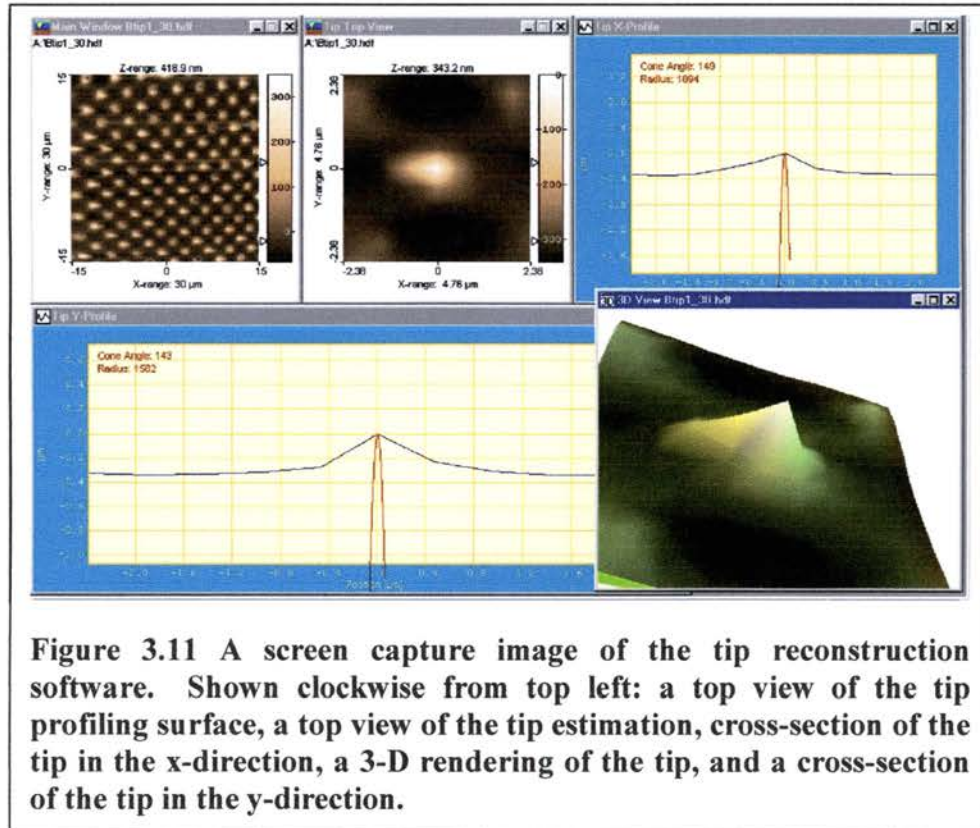
grains were very small compared with the copper, the decision was made to try sputtering the aluminum onto the tips themselves.

A complication of this process was that in preliminary trials with coating the tips with aluminum oxide, it was found that the Al_2O_3 coating caused the cantilever chips to “curl”, making focusing the laser on the back of the cantilever chip difficult. To help address this problem, a thin layer of aluminum was sputtered before depositing the aluminum oxide layer. Another concern of this portion of the project was the thickness of the layers deposited onto the tips. Films that are too thick or not evenly distributed onto the cantilevers may affect the radius of curvature of the tip. To measure the thickness of the two layers, a small cutting of a flat silicon wafer was sputtered along with the cantilever chips.

A profilometer was used to measure the thickness of the aluminum seed layer and the aluminum oxide film deposited on the silicon wafer. The seed layer was found to be about 5 nm thick, and the aluminum oxide layer to be 8.5 nm. Since the radius of curvature of the Ultralever tip is only 50 nm, a concern of this process was that depositing an additional 13.5 nm of material on the tip might make it too blunt for useful AFM imaging. To test this, both coated and uncoated tips were used to image a tip-profiling surface (pictured in section 3.4.1), and these images were loaded into “blind reconstruction” software.

Two of each type of tip were tested, and these preliminary tests showed that the coated tips were in fact comparable to the uncoated tips both in radius of curvature and tip cone angles. This suggests that the sputtering process was successful in distributing the aluminum and aluminum oxide coatings evenly over the surface of the tips. It also

suggests that using Ultralever tips coated with aluminum oxide may in the future be useful for more closely modeling the CMP process with the Atomic Force Microscope.



CHAPTER FOUR

CONCLUSIONS

4.1 Comparison of *Ex Situ* And *In Situ* Experiments

There are several fundamental differences between the *ex situ* and *in situ* experiments that make it difficult to make a direct comparison of RMS roughness values. The primary difference between the two is that while the copper films polished in the commercial polisher were abraded by many particulates and exposed to the corrosive solution for a relatively short amount of time (5 minutes), the copper films “polished” with the AFM were abraded by only one particulate (the AFM tip) and exposed to solution for a much longer period of time (about 1.5 hours). Despite this difference however, it is important to note that in both of these types of trials, similar trends were recorded relating the pH of the polishing solution and the smoothness of the polished copper sample. In both the *ex situ* and *in situ* trials, it was observed that the solutions with a lower pH level (more acidic) were much more successful in planarizing the surface than the solution had a pH close to being neutral. In fact, in both cases, the solution at pH 6 processed samples to be only slightly smoother than the unpolished “as received” samples.

The major difference between the two trials was that while the *ex situ* trials seemed to suggest that the relationship between pH and planarity may be a bell-shaped

curve, with a moderately acidic solution being more successful than a very acidic or neutral solution, the *in situ* trial did not seem to concur with this theory. It may be found with future improvements to the AFM system, such as tip coating, that a more meaningful determination of which solution is more successful will be found.

Despite this small disparity between trials however, it should be noted that the data from both the *in situ* and *ex situ* experiments suggest that pH may indeed be an important factor in polishing copper with CMP. As has been mentioned, in both types of trials it was shown that copper thin films polished with solutions of low pH were significantly more planarized than films polished with a less acidic solution. Similarities between the trials also suggest that the Atomic Force Microscope may be a useful tool in exploring the fundamental mechanisms of Chemical Mechanical Polishing.

4.2 Suggestion for Future Works and Other Projects

Because of the high number of variables involved with the AFM-CMP simulation, there are almost unlimited choices for future studies in this area. Other ways to explore this topic include investigating the effect of more basic solutions on the polishing process, varying the concentration of corrosion inhibitor in the solutions, and studying the effect of different parameters of the AFM such as scan rate, pressure, and exposure time. The concentration of corrosion inhibitor may be particularly relevant to studying not only surface planarity, but also material removal rates. In addition, a number of improvements can be made to the system to enable the AFM to more accurately model the CMP process. The preliminary data given in 3.4 suggests that using AFM tips coated with alumina may allow the tip to more closely model an actual polishing particulate. Another

improvement that may be useful to this project would be to introduce a small pump system into the microcell. In an actual polisher, the polishing slurry used to smooth the copper is continuously refreshed; meaning that slurry, once dense with copper particles, is swept away and fresh slurry is introduced. The data obtained for section 3.3 (*in situ* experiments) indicates that as the corrosive liquid stays on the surface (trapped in the microcell) for a long period of time, the RMS roughness of the sample begins to rise again after being polished. One possible source of this inconsistency may be that the fluid is contaminated with free copper particles, which re-adhere either to the tip or to the sample. Thus it is possible that the addition of a pumping mechanism to refresh the fluid would greatly improve the microcell system. Another reason that the addition of a pump would be useful is that it might help correct the scan problems experienced in the microcell experiment, most likely due to thermal drift.

Besides these suggestions, another possible experiment that would be relevant to this project would be to do a similar analysis, both *ex situ* and *in situ*, of patterned surfaces composed of both copper and a low-k dielectric. As was described in Chapter 1, choosing an appropriate dielectric for the areas between copper lines has become increasingly important as device sizes have decreased. Therefore another possible project similar to this one would be to study the possibility of whether the AFM could be used to polish a combination of both copper and a low-k dielectric. In this way the project would more accurately model the actual IC manufacture process, in that the two materials are most likely to be located on the same plane when polished.

BIBLIOGRAPHY

- [1] <http://www.infoplease.com/ce6/sci/A0825307.html>.
- [2] <http://innovations.copper.org/cowie/bigblue.htm>.
- [3] B. Nelson, "Copper Chip could mean faster, cheaper computers," 1997, <http://www11.cnn.com/TECH/9709/22/ibm.chip/index.html>
- [4] M. Afnan, S. Chiao, M. Rehayem, P. Yih, D. H. Wang, "Stress-free polishing advances copper integration with ultralow- k dielectrics," 2001, <http://sst.pennnet.com>.
- [5] I.B. Bhat, H. Cui, S.P. Murarka, H. Lu, W. Li, W. Hsia, W. Catabay, J. Electrochemical Society, 147, 10, 3816 (2000).
- [6] J. Serda, "CMOS Progress Overview," 1999 (AMD Learning Module).
- [7] D.L. Hetherington, Y. Strausser, "Atomic Force Microscopy Measurements in Support of CMP," 1996, <http://www.di.com/Appnotes/CMP/CMPMain.html>.
- [8] D. Devecchio, P. Schmutz, G.S. Frankel, *Electrochemical and Solid State Letters*, 3, 90 (2000).
- [9] T. Cunningham, D. Dawson, L. Ge, M.G. Heaton, F.M. Serry, "Atomic Force Profilometry," 1998, <http://www.di.com/AppNotes/Vx/vxmain.html>.
- [10] H. Y. Nie, "A Brief Note on Scanning Probe Techniques," 2001, <http://publish.uwo.ca/~hnie/spmman.html>.
- [11] R. Wiesendanger, Scanning Probe Microscopy: Methods and Applications (Cambridge University Press, NY, 1994).
- [12] H. Ibach, H. Luth, Solid-State Physics (Springer-Verlag, NY, 1981).
- [13] A. Rex, S. T. Thornton, Modern Physics for Scientists and Engineers (Saunders, FL, 2000).
- [14] D. Sarid, Scanning Force Microscopy (Oxford University Press, NY, 1994).
- [15] "A Practical Guide to Scanning Probe Microscopy", <http://www.topometrix.com/spmguide>.

- [16] H. Li, "The Atomic Force Microscope," 1997,
<http://www.chembio.uoguelph.ca/chm729/afm/force.htm>.
- [17] P. Markiewicz, "The Atomic Force Microscope," 2000,
<http://www.weizmann.ac.il/surflab/peter>.
- [18] R. Jaeger, Introduction to Microelectronic Fabrication, Vol. 5 (Addison-Wesley, MA, 1988).
- [19] <http://www.lbl.gov/Science-Articles/Archive/integrated-circuits-copper.html>.
- [20] <http://www.technion.ac.il/technion/materials/eizenberg.html>.
- [21] <http://news.com.com/2100-1001-273620.html>.
- [22] M. Lim, S. Perry, H. Galloway, D. Koeck, J. Vac. Sci. Technol. B 20, (2), 575 (2002).

VITA

Kelly Marie Fishbeck was born in Austin, Texas, on July 29, 1975, the daughter of Mickey Jean Fishbeck and Robert Wilton Fishbeck, and has a sister, Casey Leigh Fishbeck. After completing her work at Crockett High School, Austin, Texas, in 1993, she entered Southwest Texas State University in San Marcos, Texas. In 1996 she was inducted into the Golden Key National Honor Society. In 1997 and 1998 she received the Department of Mathematics Award for Scholarship. In 1998 she received the Department of Mathematics Scholarship for Outstanding Achievement, was listed in the Southwest Texas State School of Science Dean's List. In December of 1998 she received the degree of Bachelor of Science in Mathematics with high honors from Southwest Texas State University. During this time she was employed at Southwest Texas State as a mathematics tutor and an undergraduate instructional assistant in mathematics. In January of 1999, she entered the Graduate School of Southwest Texas State to pursue a Master of Science degree in Physics. During this time she has worked as a graduate instructional assistant in Mathematics, a laboratory instructor in Physics, and also as a research assistant in Physics under the supervision of Dr. Heather Galloway.

Permanent Address: 1108 Radam Circle

Austin, Tx. 78745

This thesis was typed by Kelly Marie Fishbeck.